Oil & Natural Gas Technology

DOE Award No.: DE-FC26-06NT42962

Integrated Reservoir Model
(Topical Report)

Characterization and Quantification of the Methane Hydrate Resource Potential Associated with the Barrow Gas Fields

Submitted by:
Petrotechnical Resources of Alaska, LLC
3601 C. Street, Suite 822
Anchorage, AK 99503

Prepared for:
United States Department of Energy
National Energy Technology Laboratory

June, 2008

Office of Fossil Energy

Topical Report:

AN INTEGRATED RESERVOIR MODEL DESCRIPTION FOR EAST BARROW AND WALAKPA GAS FIELDS, ALASKA

June 2008

Under

CHARACTERIZATION AND QUANTIFICATION

OF THE METHANE HYDRATE RESOURCE POTENTIAL ASSOCIATED WITH THE BARROW GAS FIELDS

DOE Project Number: DE-FC26-06NT42962

Awarded to

North Slope Borough, Alaska

Project Director/Manager: Kent Grinage

Principal Investigator: Thomas P. Walsh

Prepared by

Manmath Panda and G. T. Morahan

Petrotechnical Resources of Alaska, LLC

3601 C. Street, Suite 822

Anchorage, AK 99503

Prepared for:

U.S. Department of Energy

National Energy Technology Laboratory

626 Cochrane Mills Road

P.O. Box 10940

Pittsburgh, PA 15236-0940

DISCLAIMER

TABLE OF CONTENTS

TABLE OF CONTENTS	**iii**
LIST OF FIGURES	**iv**
EXECUTIVE SUMMARY	**1**
INTRODUCTION	**1**
OBJECTIVES	**3**
BACKGROUND	**3**
RESERVOIR CHARACTERIZATION AND SIMULATION	**9**
RESERVOIR MODEL BUILD – Barrow Gas Reservoir	**9**
STEP-BY STEP DETAILED PROCEDURE OF BUILDING A 3D GEOLOGICAL MODEL	**11**
RESERVOIR MODEL BUILD – Walakpa Gas Reservoir	**31**
CONCLUSIONS	**37**
REFERENCES	**38**

LIST OF FIGURES

Figure 1: Location map for the Barrow Gas Fields **4**

Figure 2: Major tectonic features of northern Alaska **5**

Figure 3: Generalized stratigraphic column for the North Slope of Alaska **6**

Figure 4: Depiction of the opening of the Arctic Ocean **7**

Figure 5: Structural interpretation of the Avak Crater area showing depth to pre-Mississippian surface **8**

Figure 6: Geostatistical model building procedure **9**

Figure 7: Top of structure of Barrow sands showing the modeling area **10**

Figure 8: Upper Barrow sand isochore **11**

Figure 9: Structural arrangement of Barrow Sands **12**

Figure 10: Wells and faults in the East Barrow Field **13**

Figure 11: Adjusting the Top of the Barrow surface to the faults **14**

Figure 12: Barrow area fault blocks **15**

Figure 13: Grid generation parameters for Barrow Sands **16**

Figure 14: Fine scale geological grid, Barrow Sands **16**

Figure 15: Geological model grid for East Barrow Field **17**

Figure 16: Sub-zones in Barrow Sands **17**

Figure 17: Sub-zones in Barrow Sands **18**

Figure 18: Blocked wells in East Barrow Field **18**

Figure 19: Blocked well data for S. Barrow 15 **19**

Figure 20: Schematic showing facies distribution **20**

Figure 21: Facies modeling work flow **21**

Figure 22: Vertical proportion curve of Barrow facies **22**

Figure 23: Facies distribution in Barrow Sands, RMS results **22**

Figure 24: Schematic showing the petrophysical modeling workflow **23**

Figure 25: Petrophysical modeling set up for Barrow model in RMS **24**

Figure 26: Porosity distribution in Barrow Sands, RMS results **25**

Figure 27: Porosity cross section through Barrow Sands, RMS results **26**

Figure 28: Permeability distribution in Barrow Sands, RMS results **26**

Figure 29: E-W cross section through the permeability model, Barrow Sands **27**

Figure 30: Schematic showing the scale up method **27**

Figure 31: RMS work flow to scale up East Barrow fine scale model **28**

Figure 32: Scaled up porosity distribution for East Barrow **29**

Figure 33: Scaled up permeability data for East Barrow Field **29**

Figure 34: East Barrow model grid cell depth **30**

Figure 35: Temperature distribution in East Barrow **30**

Figure 36: Water saturation distribution in the East Barrow Field 31
Figure 37: Areal extent of Walakpa geological model 32
Figure 38: Facies distribution in Walakpa Sands 33
Figure 39: Porosity distribution in Walakpa Sands 33
Figure 40: Permeability distribution in Walakpa Sands 34
Figure 41: Sub-grid covering Walakpa Gas Field 35
Figure 42: Porosity distribution in Walakpa reservoir 36
Figure 43: Permeability distribution in Walakpa reservoir 36
Figure 44: Water saturation distribution in Walakpa reservoir 37

EXECUTIVE SUMMARY

This Topical Report details the reservoir characterization and model builds for the East Barrow and Walakpa Gas Fields in support of full-field history matched production simulation of the two fields. As far as we are aware, this is the first study to include integrated reservoir characterization, geostatistical simulation, and full-field history matched dynamic modeling to quantify effects of hydrate dissociation on free gas production.

This modeling effort was completed as part of a larger phased study to characterize and quantify the hydrate resource potential of the Barrow Gas Fields (BGF's).

Output from the model was primarily intended to support dynamic reservoir simulation; however, the fine-scaled geostatistical reservoir characterization also allowed for volumetric estimation of in-place free gas and hydrate resource.

The geology of the East Barrow Gas Field is more complex structurally and stratigraphically than that of the Walakpa Field, and the reservoir characterization of East Barrow relies more heavily on indicator simulation to populate the model.

This report provides some background on the geologic context for the Barrow and Walakpa sandstone formations, and describes the detailed steps involved in building the integrated geostatistical reservoir model for the East Barrow and Walakpa Fields. A companion topical report describes the reservoir simulation modeling procedure and results.

INTRODUCTION

Hydrate bearing sands are commonly encountered within and beneath the permafrost in the North Slope of Alaska and elsewhere in the arctic. Methane gas in the form of hydrates represents a tremendous resource globally, and is of considerable importance in Alaska's arctic. Economic development of these sands is challenging, since the mechanism involved in the hydrate dissociation can be significantly influenced by reservoir complexities.

While methane hydrate phase behavior is predictable in the controlled laboratory environment, complexities associated with reservoir heterogeneity, mineralogy, pore space configuration and pore-filling gas and fluid composition make formation and dissociation of in situ hydrates far more difficult to predict or explain. In order to understand the depletion mechanisms associated with production of gas from hydrate deposits, one must integrate the known properties and behavior of the hydrate being studied, with the detailed reservoir mineralogy, pore space geometry, pore fluid composition and saturation, wetability, etc. In other words, a very detailed reservoir characterization is required to effectively model response of the system to changes in pressure, temperature, and pore fluid composition. Empirical measurement in the field is a costly undertaking, and laboratory investigation, numerical modeling, reservoir characterization and dynamic reservoir simulation have been extremely valuable in supporting field investigations of in situ hydrates.

Work completed in Phase 1A of this study included methane hydrate stability modeling of the East and South Barrow and Walakpa Gas Fields. While the modeling indicated that hydrate would not be expected to be associated with the South Barrow Gas Field, the East Barrow and Walakpa Fields are believed to be capped by hydrate accumulations, based on this modeling.

The East Barrow reservoir, with an estimated GIP of 40 BCF, was discovered in the late 1940's by the U.S Navy, and is an important source of natural gas for the City of Barrow. The field currently has 7 wells capable of production. The field is road-accessible year-round, and is considered to represent a good opportunity for expansion of wellbore capacity and gas supply to Barrow, if the presumed hydrate cap at the crest of the field is capable of contributing to production of methane. Economics justify a single horizontal well or up to 5 conventional wells for future exploitation of these reserves. For production to gain the most benefit from the gas hydrate dissociation front, the location of the new wells is critical. Well performance will also depend on rock quality, structural style as it impacts fluid flow, and proper reservoir management.

To further evaluate the resource potential of hydrates associated with the BGF's, a comprehensive reservoir characterization was completed. A detailed and integrated geological study was conducted to assess the paleo-depositional system and current poro-perm details associated with the Barrow and Walakpa Sandstones.

Seismic analysis helped determine the impact of faults on sand continuity, and defined the basic configuration of the "tank". Integrating all available seismic data and logs from existing wells, a fine scale geostatistical reservoir model was constructed, which formed the basis for numerical flow simulation. A large number of simulation models, or realizations of the reservoir model incorporating major parameter uncertainties were generated. Flow simulation using these models provided data for reservoir benefit analysis, in which production forecasts were generated for various wellbore configurations.

Based on the analysis of the simulation results, a single horizontal producer is recommended in the East Barrow reservoir to allow for production of high rates of free gas at low draw-down pressures to induce dissociation of hydrates at the interface between free gas and hydrate.

This report focuses on the 3D geologic model build and a companion report describes the flow simulation work.

OBJECTIVES

- o Build fine scale Geological Reservoir Models for the Barrow and Walakpa gas reservoirs detailing:
    - • 3D reservoir configuration
    - • Facies
    - • Porosity
    - • Permeability
    - • Pore fluid/gas/hydrate saturation
- o Provide a model for reservoir simulation
    - • Create a Simulation Grid
    - • Upscale and Export Simulation Parameters for Input to Reservoir Dynamic Simulation
- o Document the complete modeling process

BACKGROUND (Extracted from the topical report on the Geological Study of Barrow Sands, Morahan, 2008)

<u>GEOLOGIC DESCRIPTION</u>

The study area for methane hydrate evaluation of the Barrow Gas Fields covers a portion of the coastal plain of the North Slope of Alaska south of the community of Barrow. It encompasses the East and South Barrow Fields, which produce from the Jurassic Barrow sandstone, and the Walakpa Field, which produces from the Neocomian Walakpa sandstone. The general area of study is shown in Figure 1.

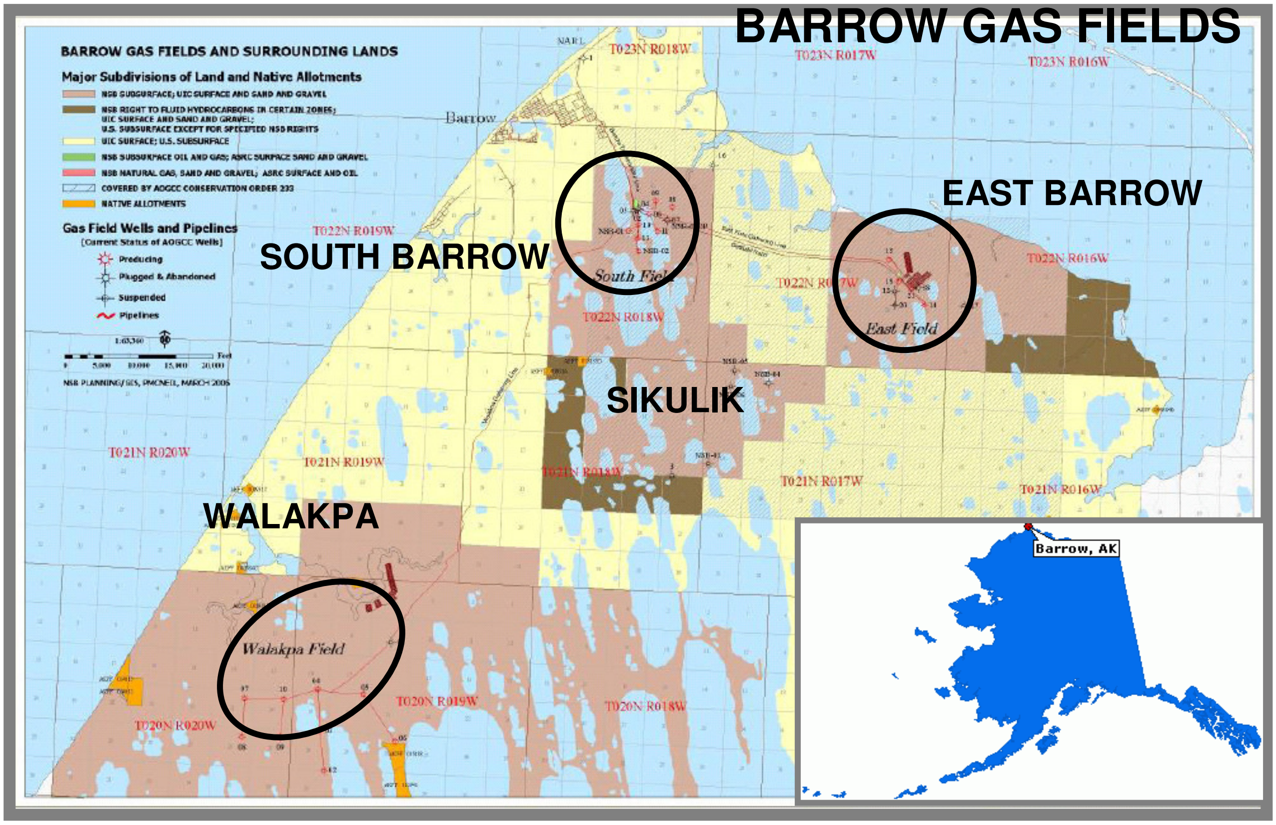

Figure 1: Location map for the Barrow Gas Fields

Geology and Tectonic Setting

The Barrow Gas Fields are located high on the Barrow Arch, a rift margin uplift that was initiated by early Jurassic time and reached maximum elevation during the Early Cretaceous with the formation of the Lower Cretaceous Unconformity (LCU), a prominent regional angular unconformity. The present day major tectonic features of the area are shown in Figure 2, and a generalized stratigraphic column is shown in Figure 3. Mississippian through Tertiary age sedimentary rocks were deposited on a deformed, intruded, and metamorphosed complex of Devonian and older rocks that are considered to be economic basement over most of the North Slope area. The post-Devonian sedimentary succession is divided by most authors into three major tectono-stratigraphic sequences, as follows:

<u>Ellesmerian</u> – Ellesmerian units form a passive margin succession that was deposited on a south-facing (present day orientation) continental margin that had been formed by Late Devonian time. The oldest and thickest Ellesmerian rocks are clastic units of the Endicott Group that were deposited within reentrants into the rifted passive margin. By late Carboniferous time carbonate units of the Lisburne Group were being deposited widely across the area and progressively overstepped the continental margin to the north. This overall onlapping pattern continued

through deposition of the clastic Sadlerochit Group, which contains the Ivishak sandstone, the primary oil reservoir within the Prudhoe Bay Field. Throughout most of Ellesmerian time the Barrow study area was either non-depositional or only very thinly covered by post-Devonian sedimentary rocks. However, by Late Triassic time the overstepping reached the southernmost portion of the study area as evidenced by thin Sadlerochit clastic units which overly the pre-Mississippian erosional surface in the Arco Brontosaraus-1 well. Over most of the study area Shublik and Sag River Formations (Fig. 4) are the only Ellesmerian units present.

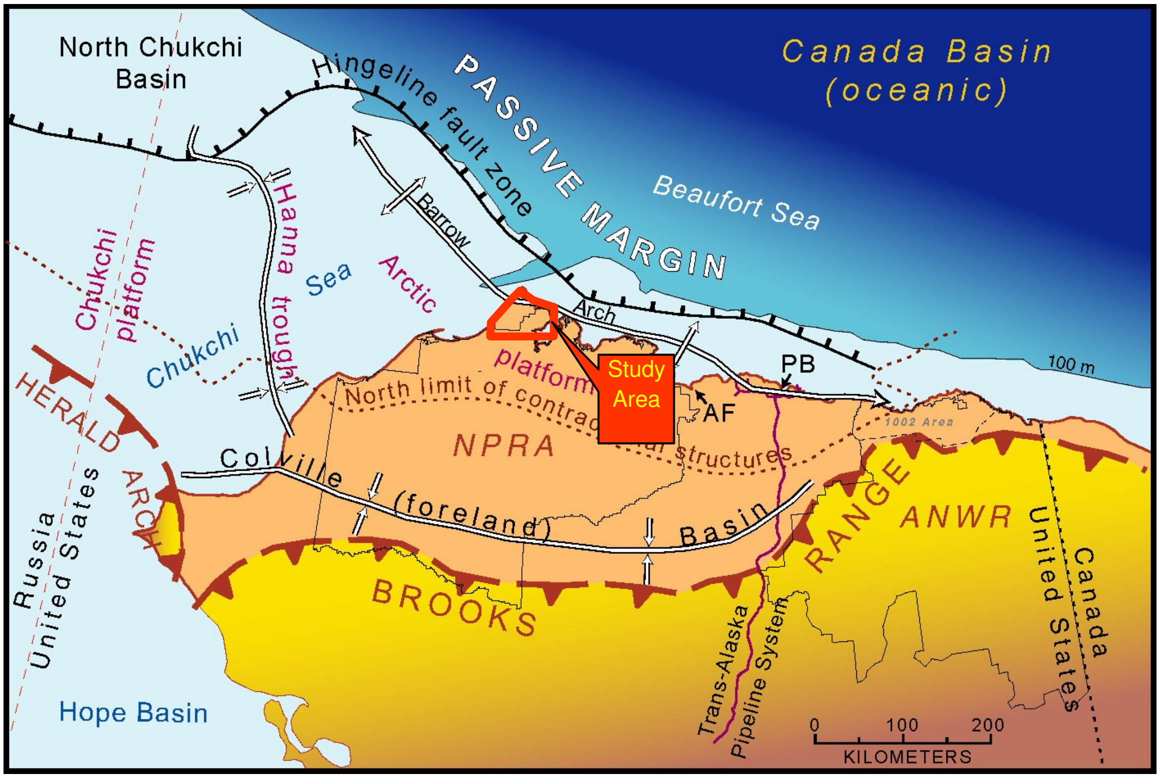

Figure 2: Major tectonic features of northern Alaska (modified from Houseknecht and Bird (2005) and Bird (2001)

<u>Beaufortian</u> – Beaufortian units form a rift-related succession of mostly clastic sedimentary rocks of Jurassic and Early Cretaceous age (Fig. 3). By early Jurassic time northwest-southeast oriented rifting had begun within what was probably a massif region to the north of the Barrow study area. The rifting progressed, and a new north-facing continental margin was formed by Early Cretaceous time along the opening Arctic Ocean. Figure 4 is an interpreted sequence of events associated with the opening. The former massif area is probably now located within the thinned and subsided transitional crust of the Beaufort Sea margin to the north of Barrow. Beaufortian rifting, uplift, and southward tilting terminated the Ellesmerian mega-transgression and created a new pattern of regressive deposition on the North Slope. Jurassic-Neocomian Kingak shale units (Fig. 3) prograded from north to south across the area in several seismically well-defined pulses and built out the continental shelf area (Houseknecht and Bird, 2004).

During Early Cretaceous time continued uplift along the Barrow Arch resulted in sub-aerial exposure and erosion of pre-Early Cretaceous units and the formation of the Lower Cretaceous Unconformity. The LCU event eroded the highest areas of the Barrow Arch down to pre-Mississippian "basement" rocks; however, within the Barrow study area erosion progressed only down to Upper Jurassic rocks, leaving Lower Jurassic and Triassic rocks preserved.

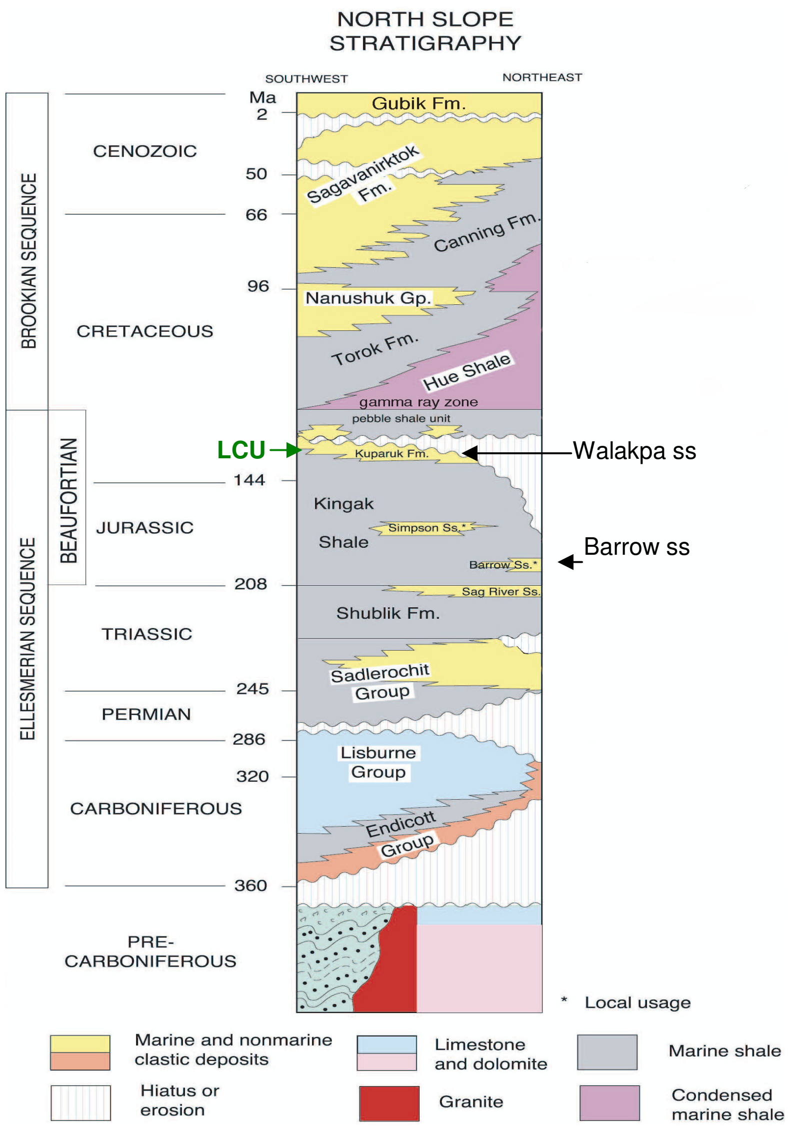

Figure 3: Generalized stratigraphic column for the North Slope of Alaska (modified from Peters, et al, 2003 and Bird, 2001)

Brookian – Following Beaufortian rifting and uplift the North Slope area came under the influence of crustal downwarping associated with development of the Brooks Range orogen to the south. By the end of Early Cretaceous time at least several thousand feet of prograding clastic shelf (Nanushuk Gp.) and slope (Torok Fm.) units had been deposited across the study area in response to uplift of the Brooks Range. Sediment transport was in a west to east direction down the axis of the developing Colville Basin (Fig. 4) and eventually overstepped the Barrow Arch to form the present day Beaufort Sea shelf (Bird, 2001).

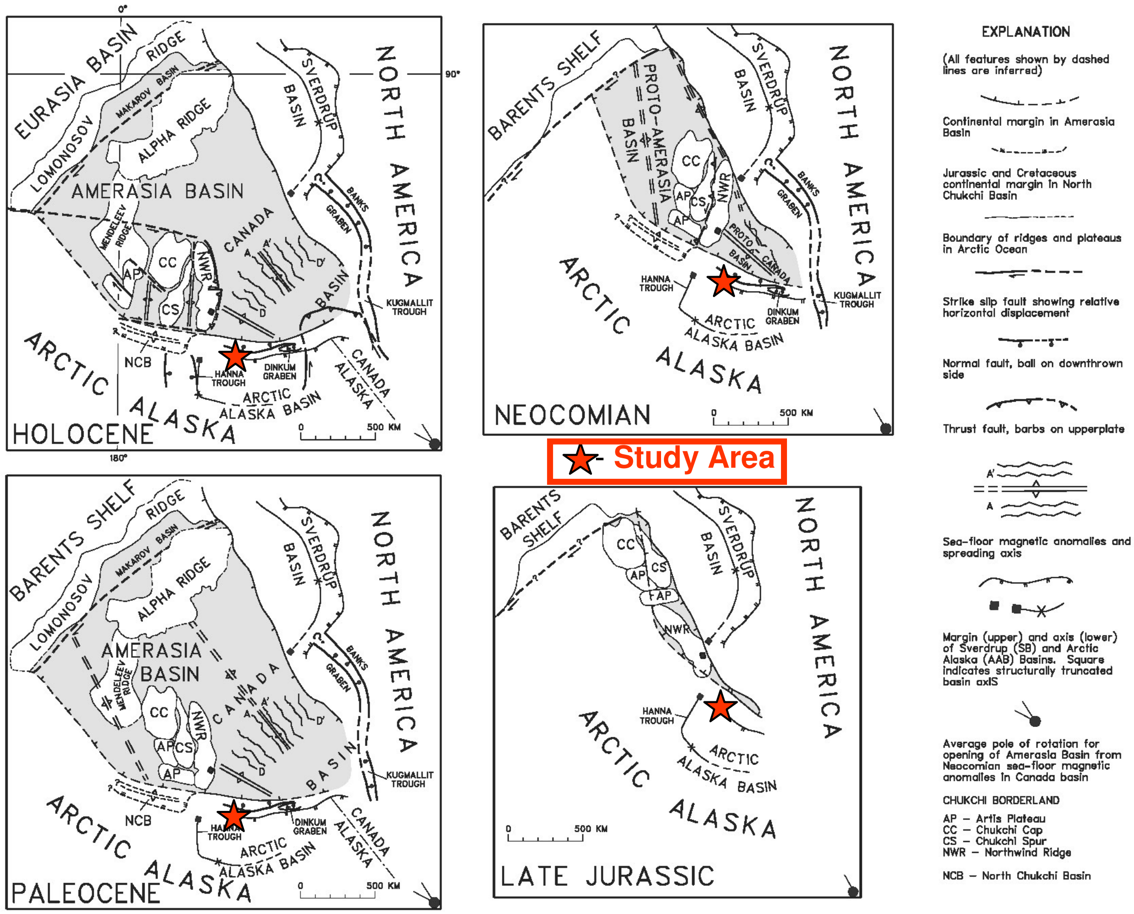

Figure 4: Depiction of the opening of the Arctic Ocean (modified from Grantz, et al, 1998)

Following deposition of the Early Cretaceous shelf and slope units two significant events occurred which contributed to the present day structural setting of the Barrow study area. One was uplift and erosion, which created a large domal feature commonly referred to as the Barrow High in the area of Barrow Gas Fields. The other was the formation of the Avak Crater, a depression and region of chaotic structural disruption that has been interpreted as an impact crater (Kirschner et al, 1992). The South and East Barrow Gas Fields, as well as the Sikulik discovery, are all on structures along the uplifted crater rim (Fig. 5). The ages of these events are not well known because the uplift and subsequent erosion has removed all pre-Holocene rocks younger than Early Cretaceous in age. The amount of post-Early Cretaceous uplift has been estimated at around 5,000 feet within the study area (Nelson and Bird, 2005).

Stratigraphy of the Barrow and Walakpa Sandstones

Barrow sandstone – The Barrow sandstone is interpreted as Early Jurassic, possibly Hettangian in age, and is part of the first cycle of Beaufortian deposition across the region. The sands are part of an overall regressive succession of clastic units that prograded from north to south across the Barrow region. Houseknecht and Bird (2004) believe that most of the sediment influx was from a point source to the north of the Barrow area. In an unpublished thin section and core analysis report (Opstad and Associates, 1989) the sandstones are interpreted to be reworked and heavily bioturbated offshore bar units. The report also notes that the reservoir quality of these sands decreases steadily to the south, away from the area of sediment influx. Given the overall pattern of Jurassic deposition within the study area it is likely that patterns of consistent reservoir characteristics will tend to line up in an east-west to northeast-southwest direction, and this is taken into account in the reservoir modeling work.

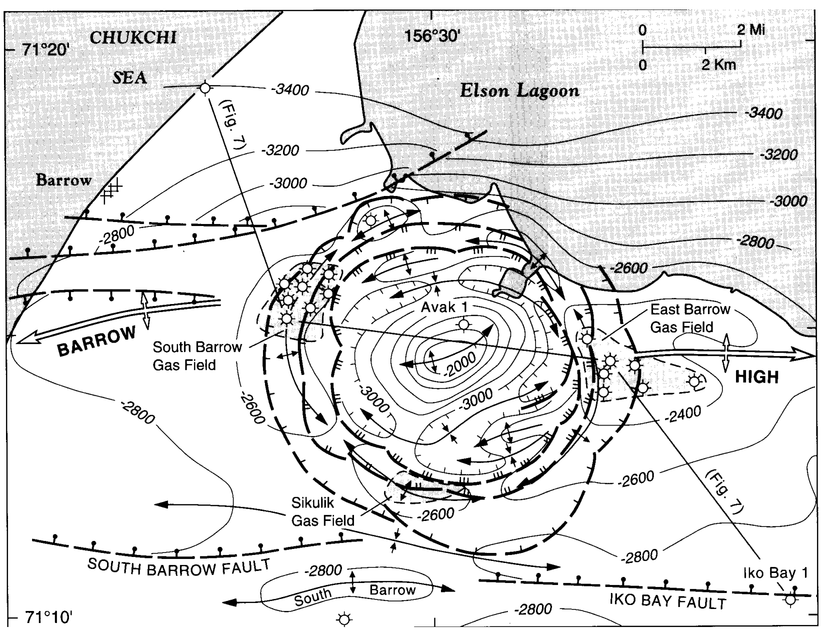

Figure 5: Structural interpretation of the Avak Crater area showing depth to the pre-Mississippian surface (from Kirschner et al, 1992)

Walakpa sandstone – The Walakpa sandstone is probably Neocomian in age, as it was deposited directly on the Early Cretaceous erosional surface (LCU) and is overlain by Neocomian to Aptian Pebble shale (Kimyai, 2000). It has characteristics similar to the trangressive Kuparuk C sandstone to the east and may be approximately the same age. The Kuparuk C was deposited within areas of accommodation space on the LCU surface and is the main reservoir within the Kuparuk Field. In addition to occurring within the Walakpa Field, the Walakpa sandstone appears to be present as a thin sand unit within the South Barrow Field, and siltstones within the East Barrow and Sikulik Fields are interpreted as lateral equivalents (Morahan, Greet and Walsh, 2008).

Stratigraphic correlation of these transgressive sands updip to the crest of the Barrow Arch has significant positive impact on the hydrate resource potential of the Walakpa reservoir.

RESERVOIR CHARACTERIZATION & SIMULATION

Presented below are the detailed accounts of the modeling undertaken to analyze the reservoir development options for the Barrow and Walakpa gas sands. Three dimensional fine scale geological models for the entire Barrow and Walakpa regions were constructed and then CMG simulation models were generated for the East Barrow and Walakpa reservoirs for the purpose of optimizing future development strategies.

RESERVOIR MODEL BUILD – Barrow Gas reservoir

A fine scale reservoir model for the Barrow gas reservoir was built using a geostatistical method. A commercially available reservoir description software RMS, marketed by Roxar, Inc., was used. Figure 6 describes the general workflow involved in a typical reservoir model building process. It is an iterative top-down process to achieve a reasonable history match.

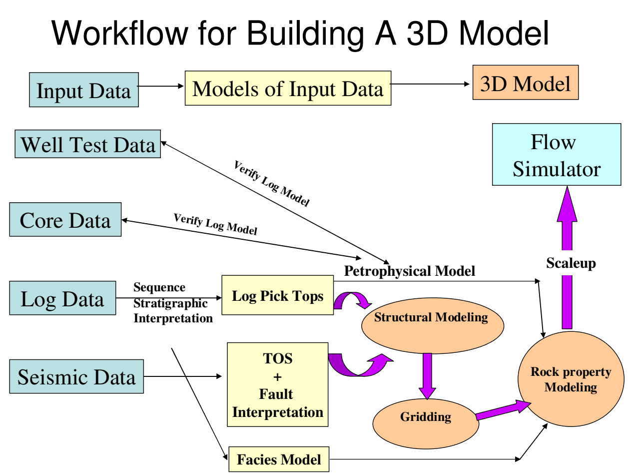

Figure 6: Geostatistical model building procedure.

Input parameters include: seismic data, well log data, core data, and well test data. Analysis of the seismic data provides the top of the structure and the maps of other horizons as well as fault information. These maps are depth-tied to the well log picks where the picks are available. Well log data and core data are used to develop well log models, such as porosity, permeability, and water saturation. These models use raw or processed log data such as the resistivity, density, gamma-ray, and neutron log to estimate rock properties along the well bore typically at 0.5 to 1 foot intervals. The gamma-ray log is also used to estimate the shale or clay content of the sand. Well test data, such as the pressure build up or RFT data are used to estimate the regional average permeability of the reservoir rock. Data from the above mentioned sources are used by the geostatistical software (RMS) to generate a fine scale model of the reservoir with petrophysical data rendered on each grid cell. The data rendering process follows a mathematical algorithm to preserve the statistical and spatial correlation of the data as exhibited by the well logs and the geological model. Fine scale models are typically scaled up to a slightly coarse simulation grid which is used to run the history match. Based on the quality of the history match the geostatistical model generation is repeated with varying parameters as input. This process is iterated until an acceptable history match is obtained.

In the following pages the above process is used to generate a geostatistical model for the Barrow gas reservoir. Figure 7 presents the areal extent of the model.

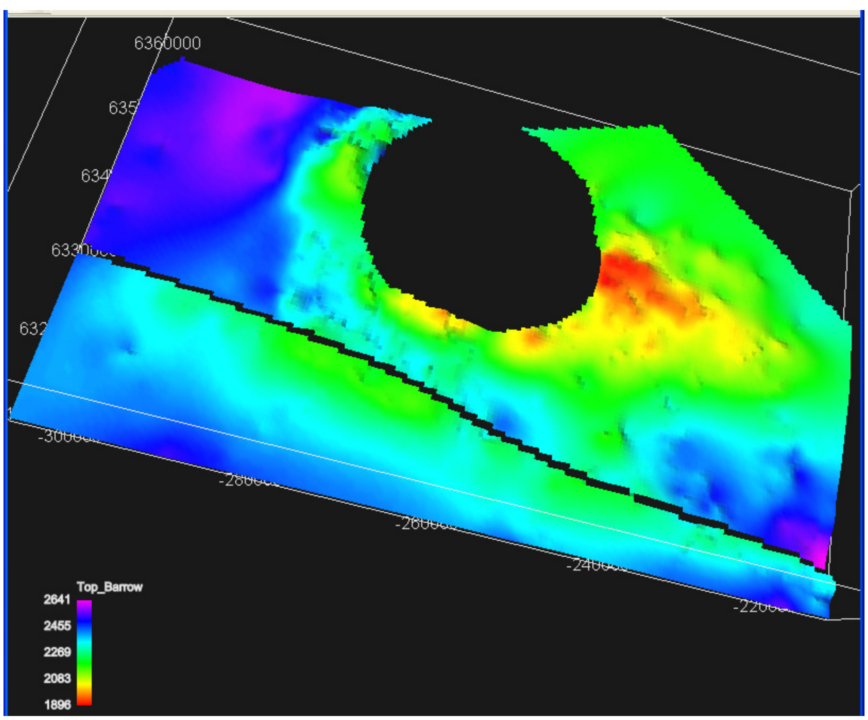

Figure 7: Top of structure of Barrow sands showing the modeling area.

THE STEP-BY STEP DETAILED PROCEDURE OF BUILDING A 3D GEOLOGICAL MODEL

<u>Step 1</u>: Import the top of the structure of the Barrow sands. This surface is obtained after analyzing the seismic data. Details of the seismic analysis are presented in an earlier topical report (Morahan, et al, 2008). Figure 7 represents the depth-structure to top of the Barrow sands. This seismically derived surface forms the top of the bulk rock or the container of the gas reservoir. Log data from 15 wells were used to condition the reservoir properties. These wells are South Barrow 9, 11, 12, 13, 14, 15, 17, 18, 19, 20, NSB -01, 02, 03, 05, and 06. Well log curves were imported into RMS from Geolog in LAS format. The imported logs are GR, NET, NPHI, RD, RHOB, SW, Por, Perm, and litho-facies The log data were also used to tie to the imported top of the structure surface.

<u>Step 2</u>: Structural arrangement – Internal surfaces of the Barrow reservoir are constructed by adding isochore maps for the upper and lower Barrow sands and the shale layer in between. These isochore maps are generated from the sand thickness data at the well locations. Figure 8. shows the isochore map for the Upper Barrow sand. A similar map was also generated for the lower Barrow sand. A constant thickness of 2 feet was used for the shale layer.

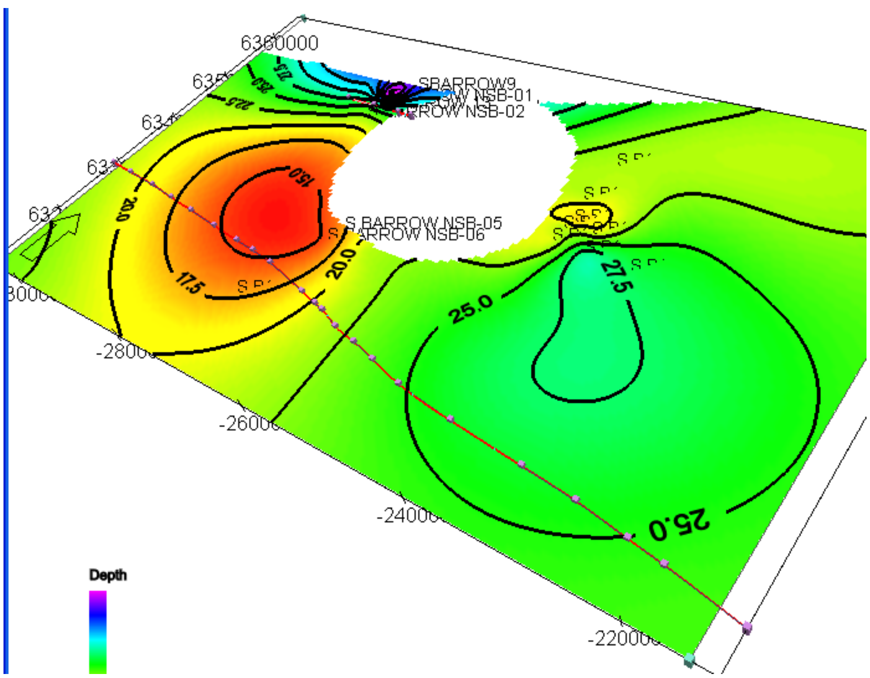

Figure 8: Upper Barrow sand isochore.

Figure 9 shows workflow of the stratigraphic framework of the Barrow sands in RMS. The top of the Barrow sands is the seismically interpreted horizon whereas the other horizons are calculated using isochore maps.

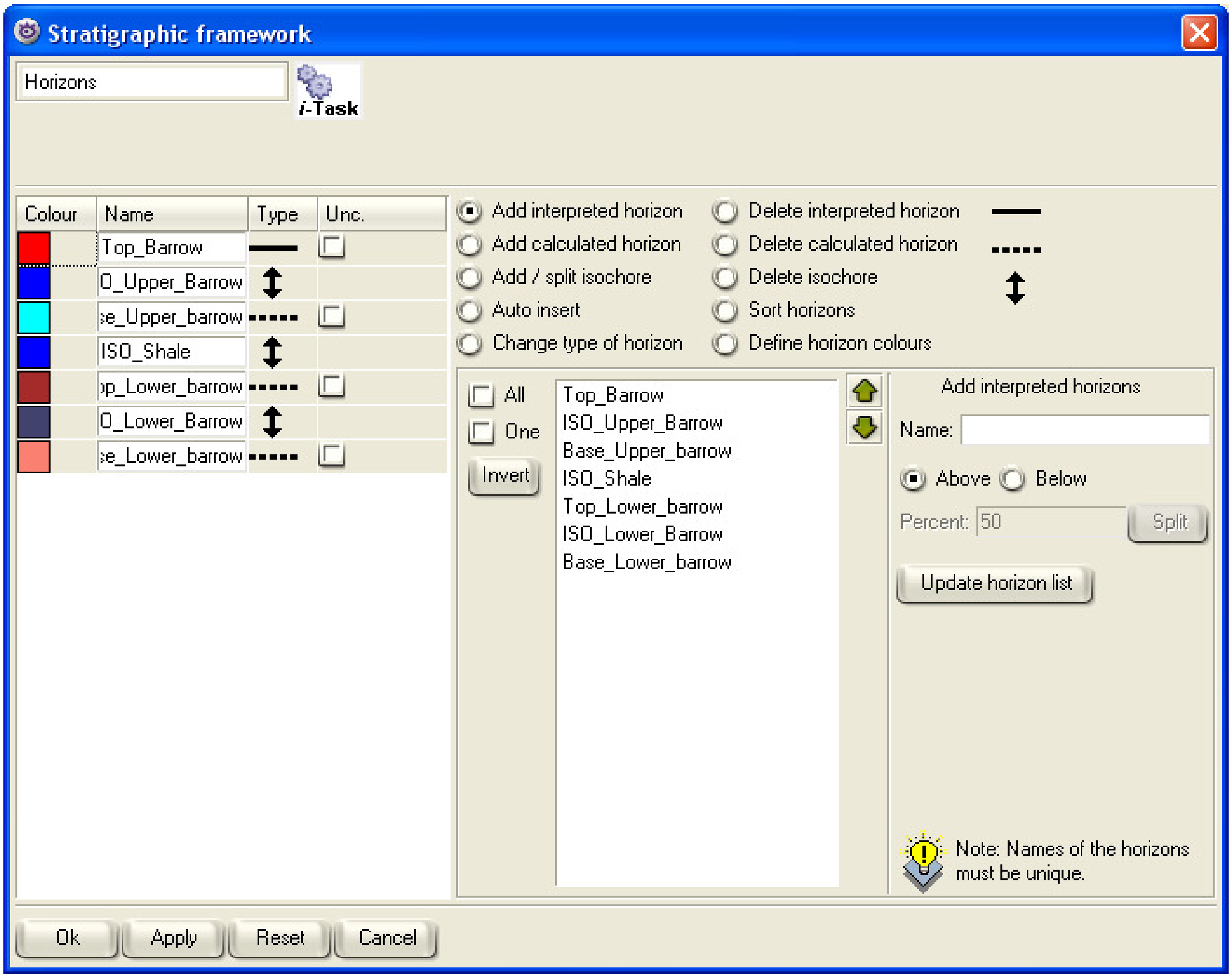

Figure 9: Structural arrangement of Barrow sands.

Step 3: Fault modeling – Based on the seismic interpretation, two faults are identified in the E. Barrow field. The fault centerlines are imported into RMS. Based on the fault throws, 2 normal faults are modeled. Figure 10 shows the faults that were modeled.

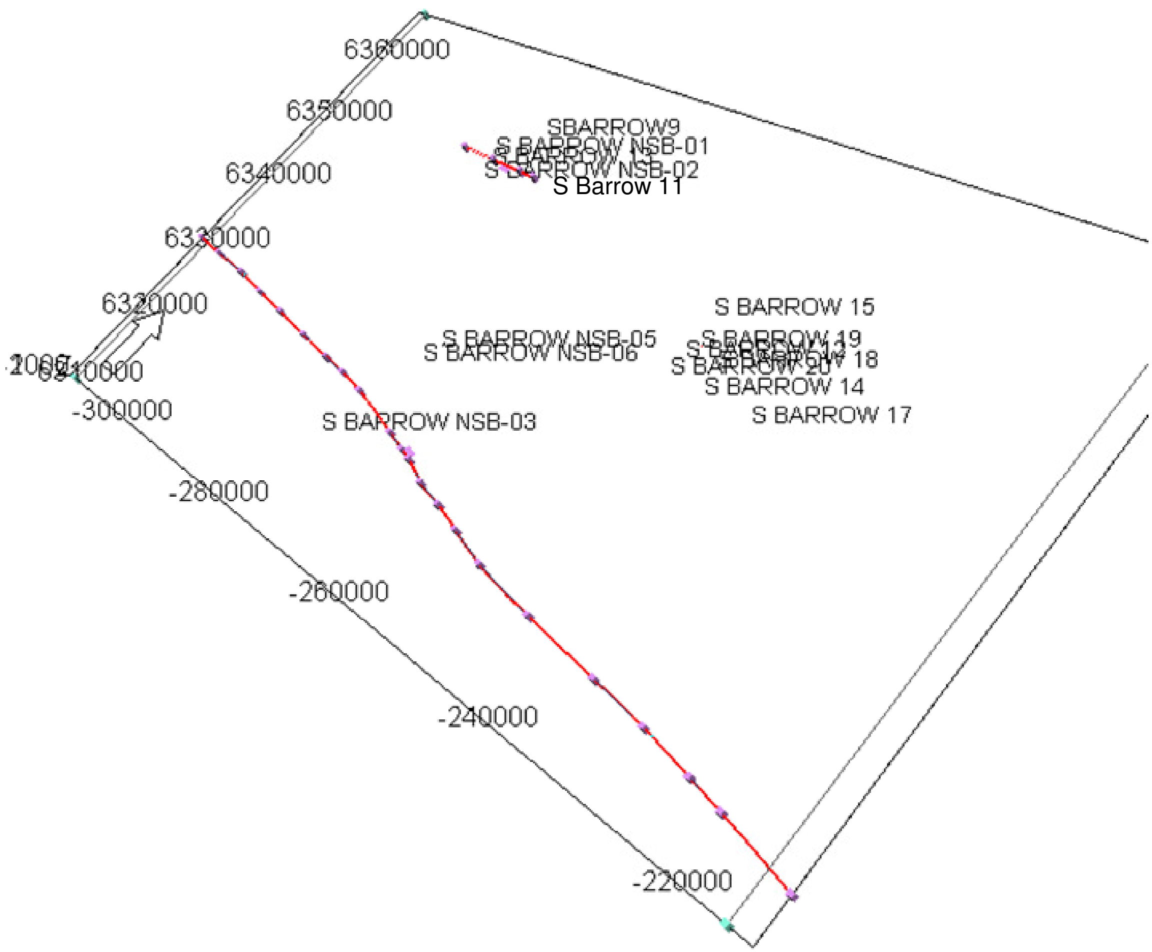

Figure 10: Wells and faults in the Barrow field.

Fault modeling is one of the critical operations in the reservoir modeling process since it determines structural arrangements and connectivity between different regions of the reservoir. In the Barrow model the southern fault divides the reservoir into two distinct regions. The southern region is downthrown into the aquifer. Gas accumulation is only in the northern region. The meteor impact crater also truncates the reservoir sand in the central region of the field.

<u>**Step 4**</u>: Horizon operation - After the fault model is completed, it is usually necessary to adjust the depth surfaces of the selected horizons to the fault model. In the Barrow model

- o RMS Fault model was used to adjust the surface and the throws on the surface to project the surface back into the fault so that it creates a tighter vertical connection

- o RMS Consistency operation was also done, this operation checks the horizons and makes them internally consistent. It is used after adjusting horizons to faults, in order to prevent any horizons from crossing each other.

- o Well correction was applied to adjust the horizon surfaces to match the z-values in all the wells using a weighted average of the input points. Influence radius of 500 ft was used within which the correction was made.

Figure 11 shows the top of Barrow horizon after adjusting to the fault.

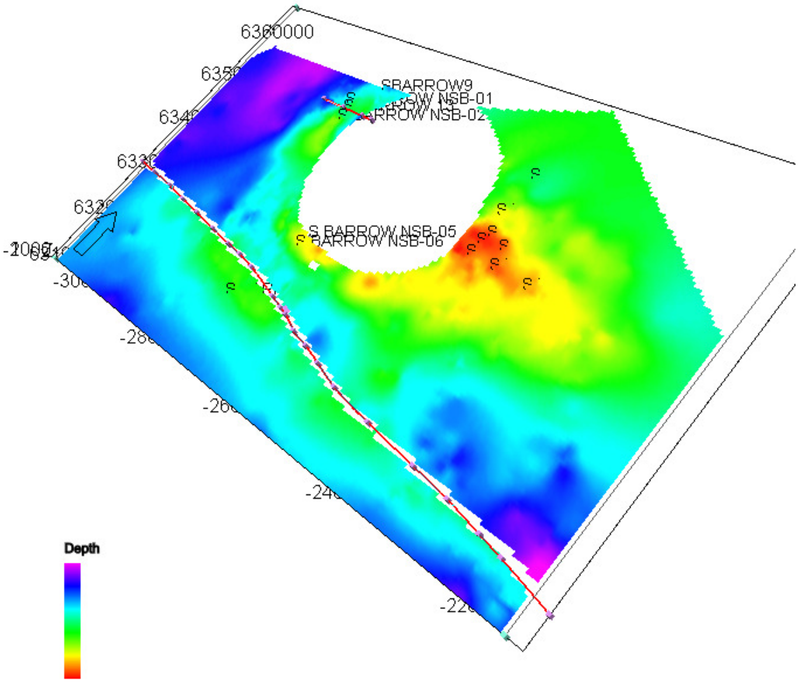

Figure 11: Adjusting the Top of Barrow surface to the faults.

The fault model splits the field into two distinct fault blocks as shown in Figure 12. Segment 1 in this figure is in aquifer zone. Free gas and hydrates only occur in segment 2.

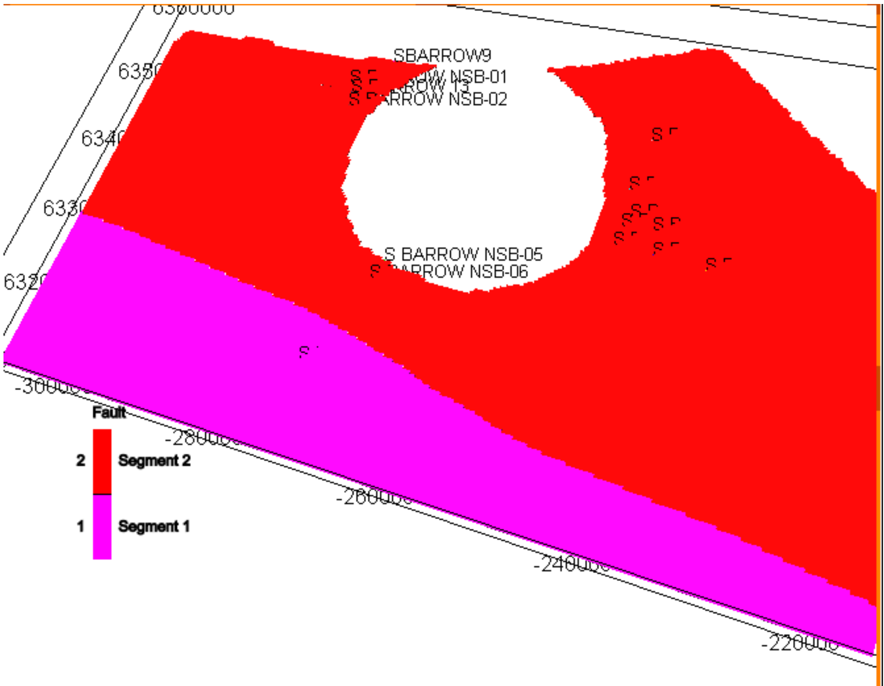

Figure 12: Barrow area fault blocks.

<u>Step 5</u>: Grid generation – Generating a 3D grid framework (also called a geologic grid) is the first step to moving into the 3D domain. It is essentially an empty framework of 3D cells, linked to the 2D horizons. The 2D horizons form the boundary of the grid, and the volume in between is filled with cells. The process after this fills these cells with values representing facies or petrophysical attributes, such as porosity, permeability, and fluid saturations.

The geological grid was created using a grid resolution of 100 feet in both X and Y directions with a uniform layering method. The grid is oriented East-West so that cells are parallel to the expected depositional strike. Using the fault model and the structure discussed in step 2 a fine scale corner point grid was generated. The grid parameters are shown in Figure 13. The Upper and Lower Barrow sands are represented by 25 and 10 layers respectively. The shale has only 1 layer.

- o (NX) 298 Columns X (NY)185 Rows (100 ft x 100 ft) - areal grid dimensions
- o (NZ) 36 layers (~2 ft) - vertical layering
- o 1.984 million total cells.

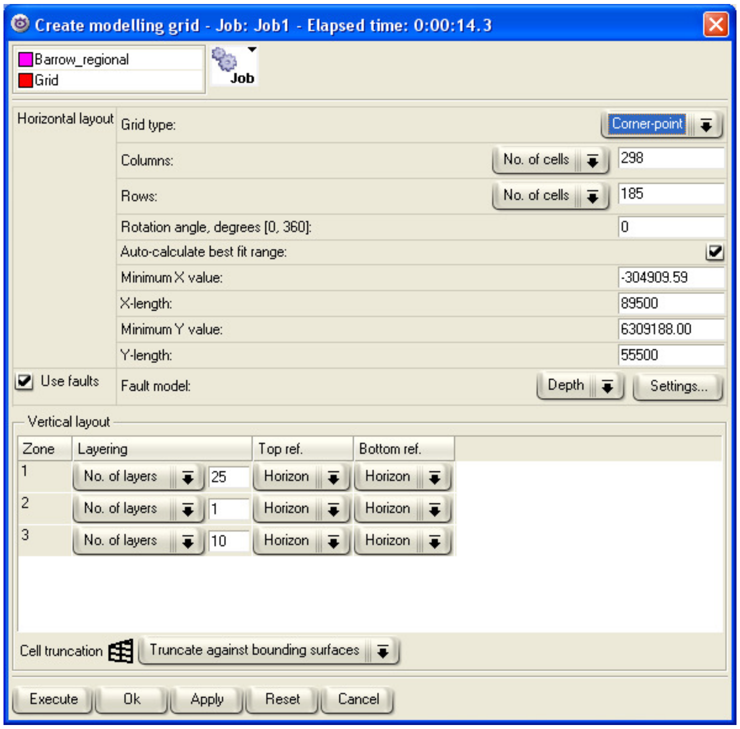

Figure 13: Grid generation parameters for Barrow sands.

Figure 14 presents the geological grid generated using the parameters in Fig. 13. The grid is vertically exaggerated to display different regions of the field.

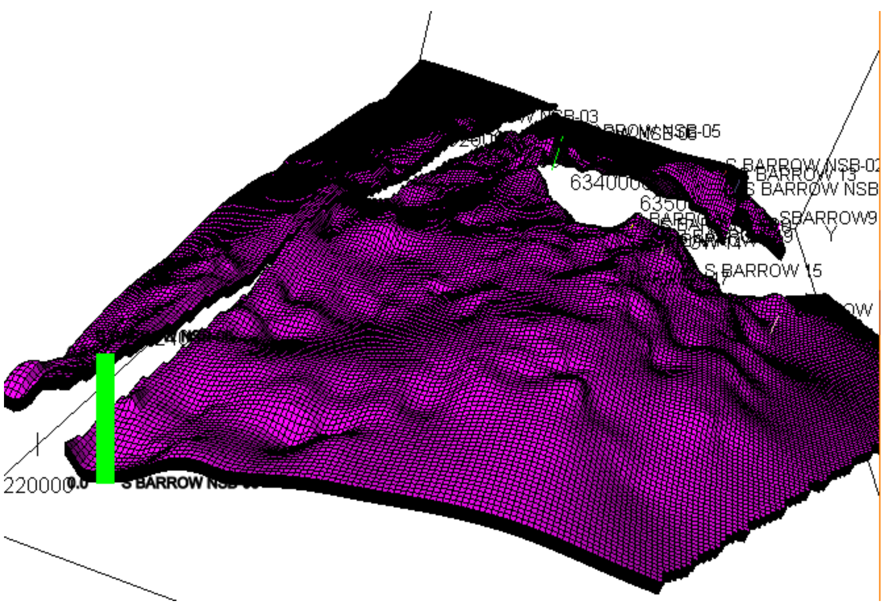

Figure 14: Fine scale geological grid, Barrow sands.

From here on the modeling is narrowed to East Barrow field, which is the scope of the flow simulation project. Figure 15 shows the geological grid for the East Barrow field.

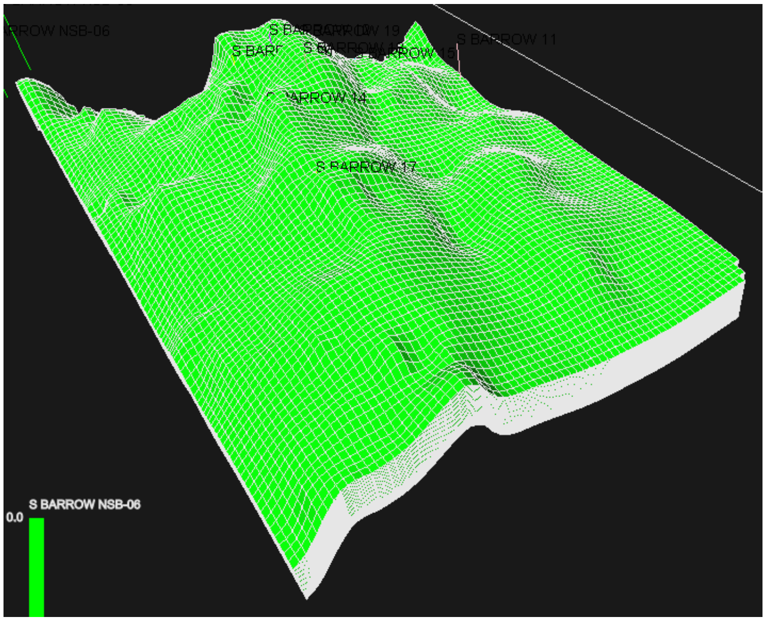

Figure 15: Geological model grid for East Barrow field.

The Barrow interval is divided into 3 zones vertically as shown in Figure 16.

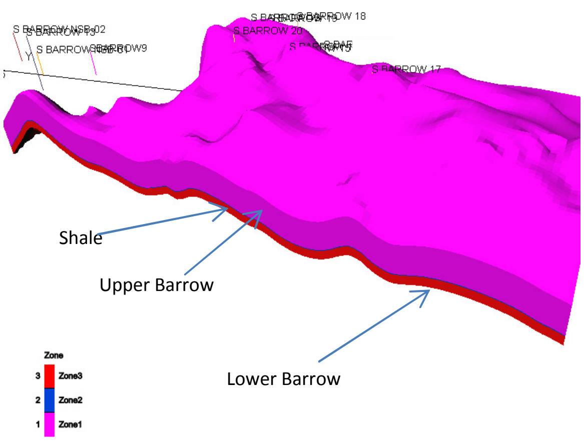

Figure 16: Sub-zones in Barrow sands.

Figure 18 presents two E-W cross sections through the model, displaying the geological zone (sub grids) and faulted area.

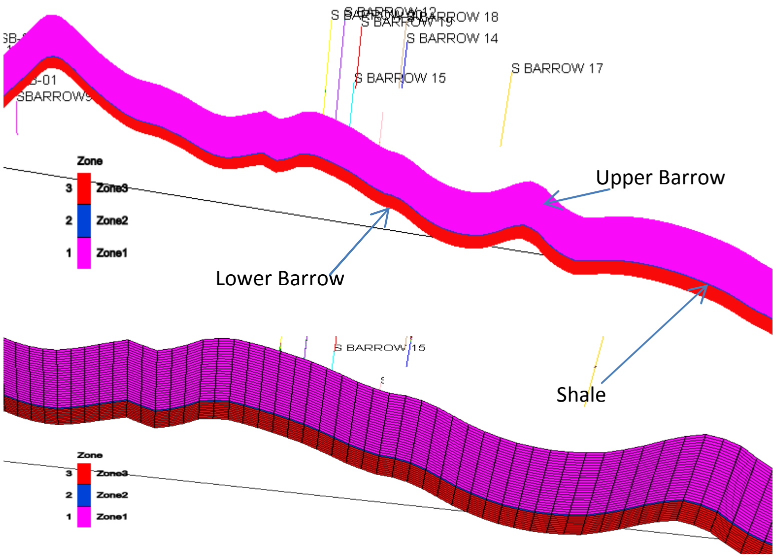

Figure 17: Sub-zones in Barrow sands.

__Step 6__: Blocking wells – After the 3D grid was built the wells were blocked from the original log curves to the resolution of the modeling grid. The up scaling method, for each selected log, is specified in the *Parameters* folder in the Block wells workflow. After they are blocked, the well logs can be visualized as shown in Figure 18. Blocked well data form the basis of the geostatistical modeling. The blocked logs (same as the well logs at the modeling grid resolution) are used as the conditioning data by the geostatistical model. Statistical analysis is also performed using the blocked well data to estimate such parameters as the mean, standard deviation, and the skewness. Spatial arrangement of the well data is estimated by performing a variogram analysis that determines how well the well log data are correlated to each other. The variogram analysis provides the values of the nugget, correlation length and the azimuth of the direction of the maximum correlation.

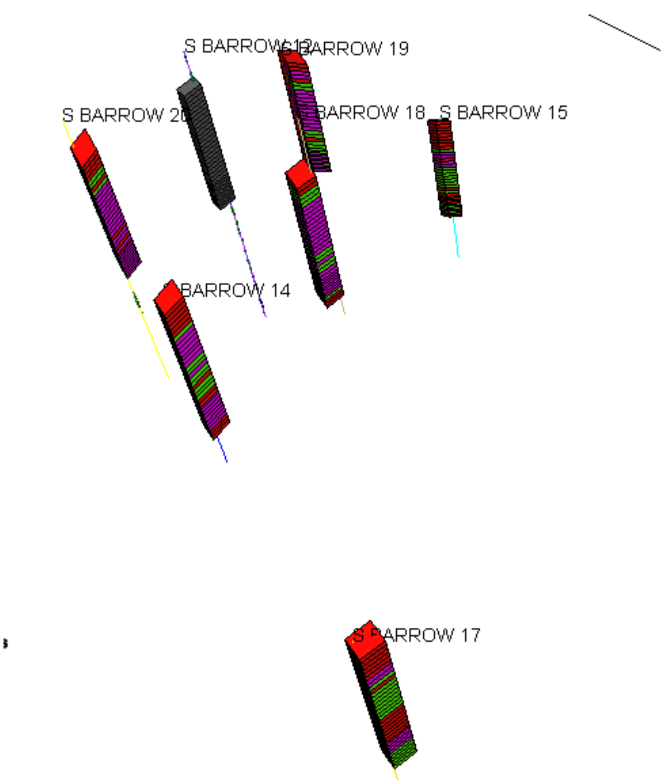

Figure 18: Blocked wells in East Barrow field.

Figure 19 presents a detailed example of the blocked well S. Barrow 15. The property displayed is the effective porosity, phie. The middle section shows both the original data as well as the blocked property curve for phie (cyan lines are the log curves: bold- blocked data, thin – original data).

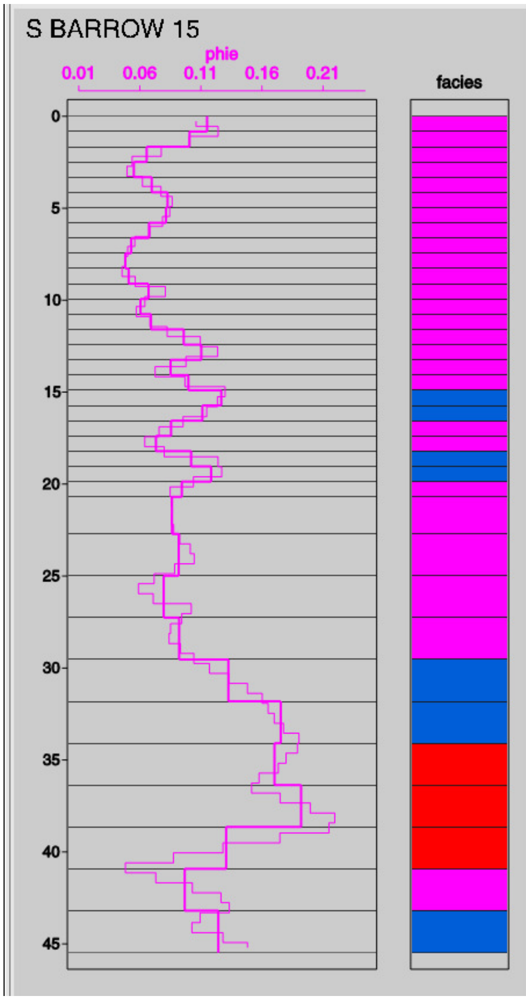

Figure 19: Blocked well data for S. Barrow 15.

<u>Step 7</u>: Property modeling - Once a 3D grid framework is constructed it is then appropriate to distribute reservoir properties such as the porosity, permeability, and fluid saturations. However, it is a standard practice to capture geological trend distribution in the reservoir first by distributing the geologic or petro facies in the model grid.

Facies Modeling –

RMS offers a number of tools for 3D stochastic modeling of facies and petrophysical parameters. These include both pixel-based (grid-based) and object-based methods for facies modeling, and Gaussian simulation method for petrophysical properties.

For the Barrow model an indicator simulation method (a pixel-based method) was used to populate the model with facies. An indicator is a stochastic pixel-based facies modeling technique that generates a discrete 3D facies parameter. The grid cells are simulated by visiting them in a random order, calculating the probability distributions, and drawing a sample at random from this distribution. For each cell, the method searches the surrounding cells for known or previously estimated probability values. These are used to estimate the current cell's probability value (for each facies), by the indicator *kriging method*. The calculation method depends on input selections. Figure 20 schematically displays how the facies distribution is used in the reservoir modeling.

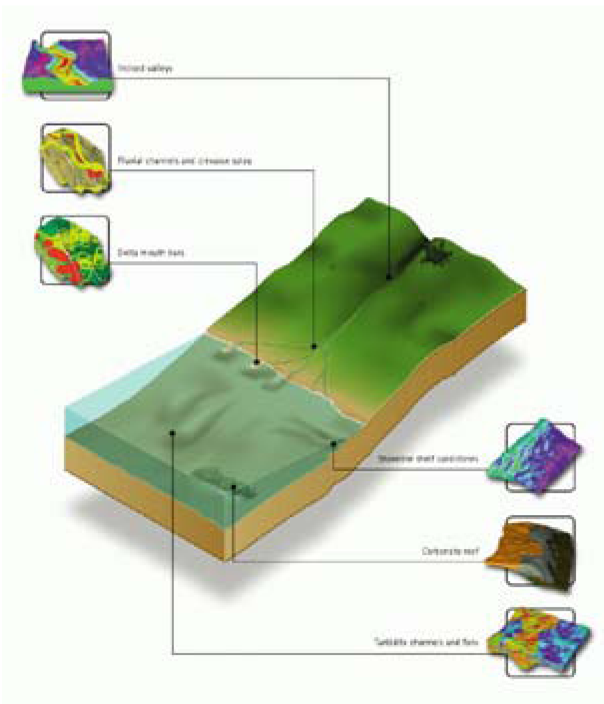

Figure 20: Schematic showing facies distribution.

For the East Barrow field facies model we used the following criteria. Figure 21 displays the RMS workflow for building the facies distribution model.

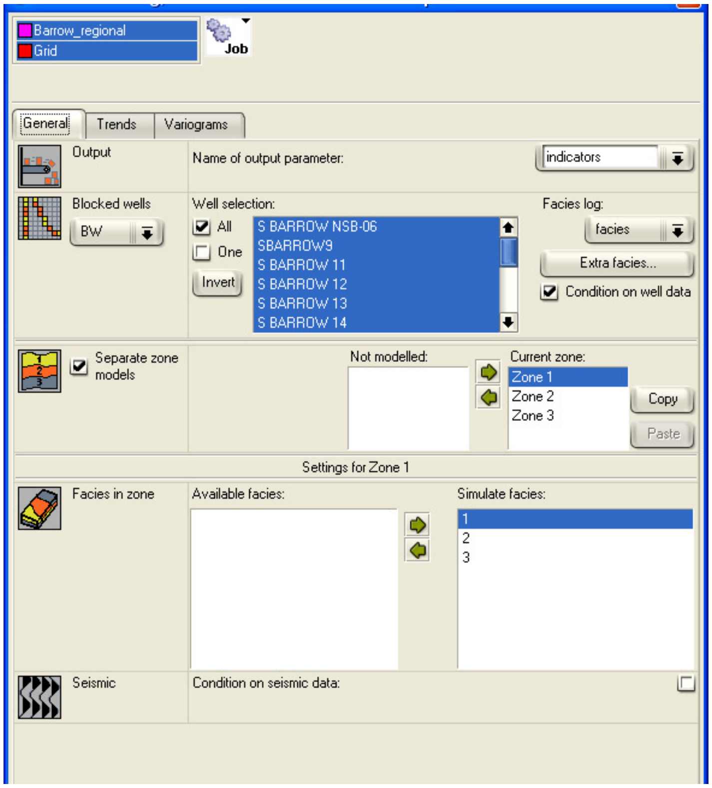

Figure 21: Facies modeling work flow.

o Facies association was defined via permeability cutoffs on Blocked wells

o In the indicator modeling step, the FACIES_DISCRETE log was used. 3D trend with 1D vertical proportion curve and Indicator variograms as input data

o For each unit in the model a different set of criteria was used for populating reservoir parameters, based on known facies correlation length and trend.

o Geologic trends were given for each facieswere used for all of the subgrids. These trends help guide the population of the facies.

o Facies correlation length, geometry and orientation were used to control the geostatistical simulations as well.

o Created Vertical proportion Curve (VPC) from block well (BW) data analysis of FACIES _DISCRETE to use as 1D trend in Indicator modeling.

The facies vertical proportion curve presented in the figure below is used for modeling facies in the Barrow sands

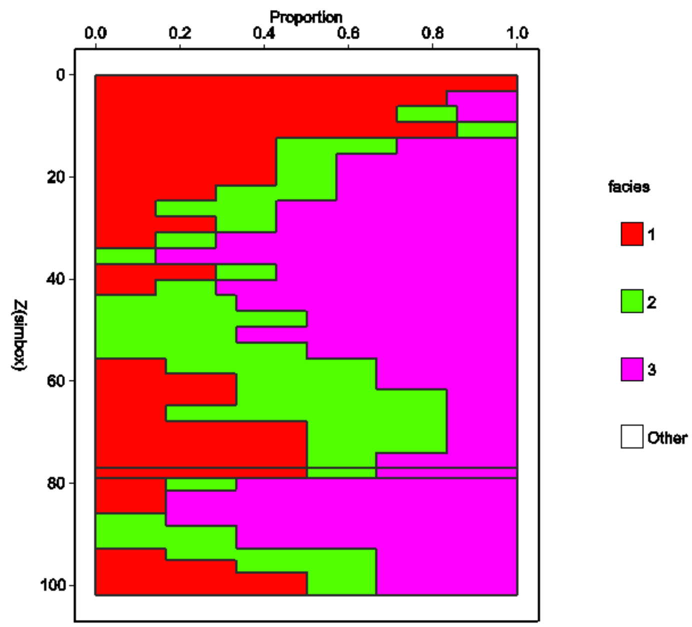

Figure 22: Vertical proportion curve of Barrow facies.

- o FACIES_DISCRETE log, 3D trend with 1D vertical proportion curve and Indicator variograms used as input data to distribute the facies in to the 3D geological grid.

The figure below presents 2 cross sections showing the distribution of facies from the 3D rendering of geologic facies in the East Barrow modeling grid.

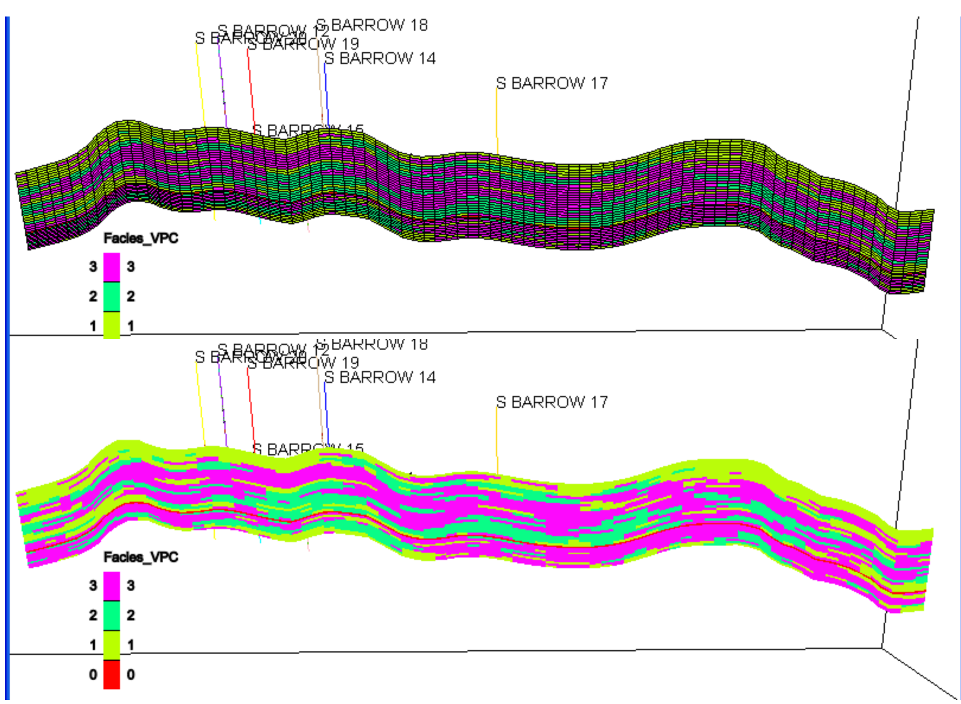

Figure 23: Facies distribution in Barrow sands, RMS results.

Petrophysical data modeling-

Observations of petrophysical parameters in a reservoir, such as porosity and permeability, are obtained from well data. The Petrophysical modeling tool in RMS allows us to generate realistic descriptions of the petrophysical parameters throughout the reservoir, based on the input data and knowledge of their trends and distributions. The modeling can be performed either deterministically or stochastically (Gaussian simulation), and conditioned to the input well data and a facies parameter. Figure 24 schematically shows the workflow of a typical petrophysical modeling method.

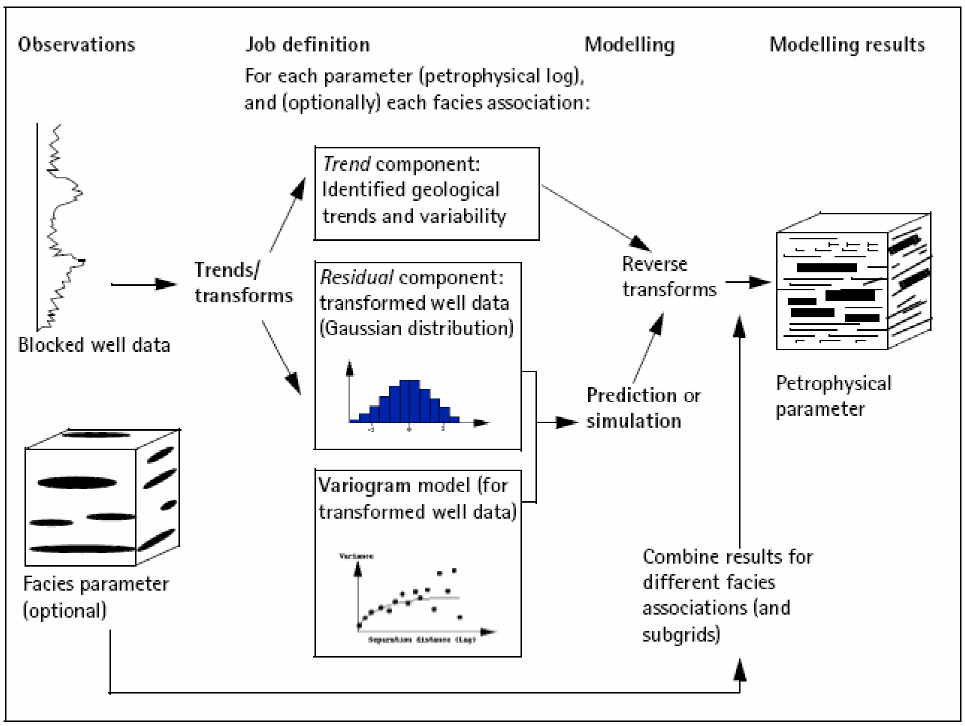

Figure 24: Schematic showing the petrophysical modeling workflow.

In addition, seismic data can be used as co-simulation parameter or seismic as a trend. The model can be defined differently for different facies and subgrids. A variogram model is used to estimate continuity in the reservoir.

In the East Barrow model a Gaussian stochastic simulation algorithm was used to produce a unique model of heterogeneity in the reservoir in terms of porosity and permeability distribution.

Porosity and permeability were conditioned to the facies distributions. To accomplish this task, a Gaussian field is simulated for each facies or rock type. This means that the whole zone is modeled to reproduce any observed relationship between measured petrophysical properties in the well logs and the interpreted facies associations.

The figure below shows RMS petrophysical modeling workflow.

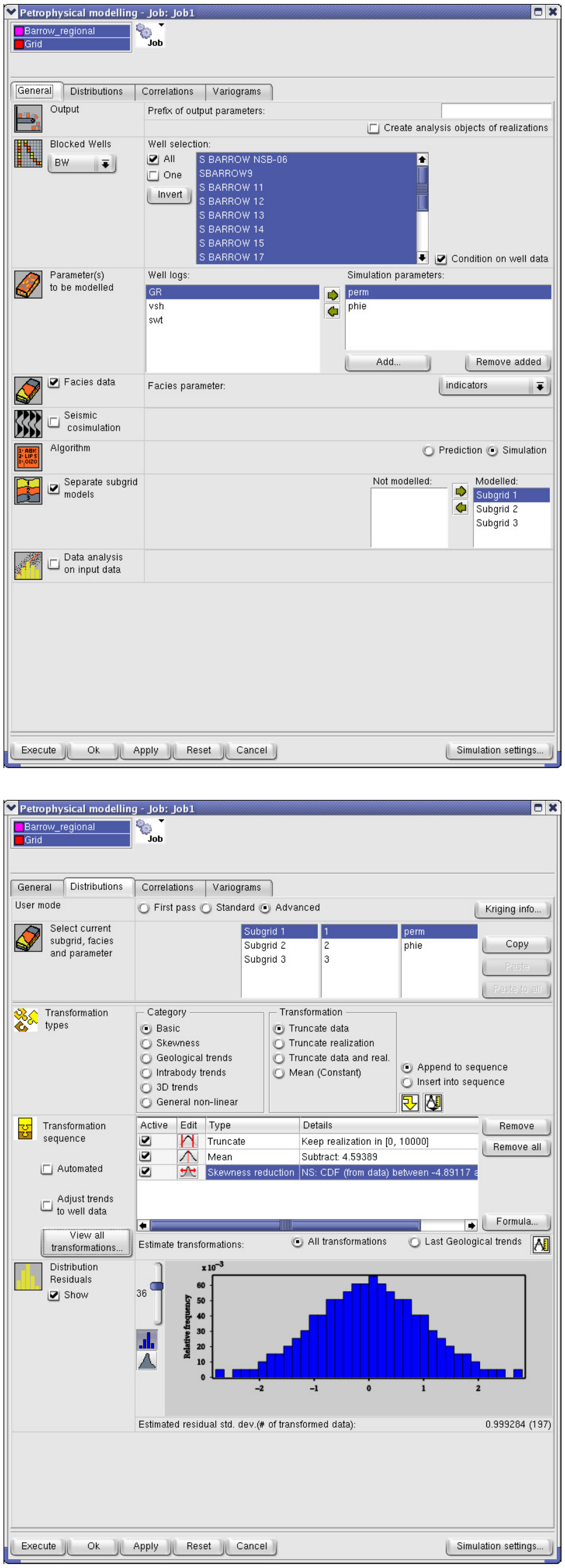

Figure 25: Petrophysical modeling set up for Barrow model in RMS.

Petrophysical properties, such as the porosity and permeability are modeled for each facies and each sub-zone separately. The generated properties are conditioned at the wells, meaning that the grid cell properties match with the well data exactly. In the interwell areas the properties are distributed according to the statistical properties of the well data. The input parameters that control the interwell property distribution are the mean, standard deviation, and skewness of the data and the data variograms, which describe the spatial correlation of the petrophysical properties of the rock. For example, a rock with a large correlation length is caused by layering where as that with a short correlation length is indicative of a random property distribution.

Results from the petrophysical modeling are presented next. Figure 26 shows the porosity distribution in Barrow sands. Average porosity increases in the lower sand and decreases towards the top of the reservoir interval (matching the trend in the well log data).

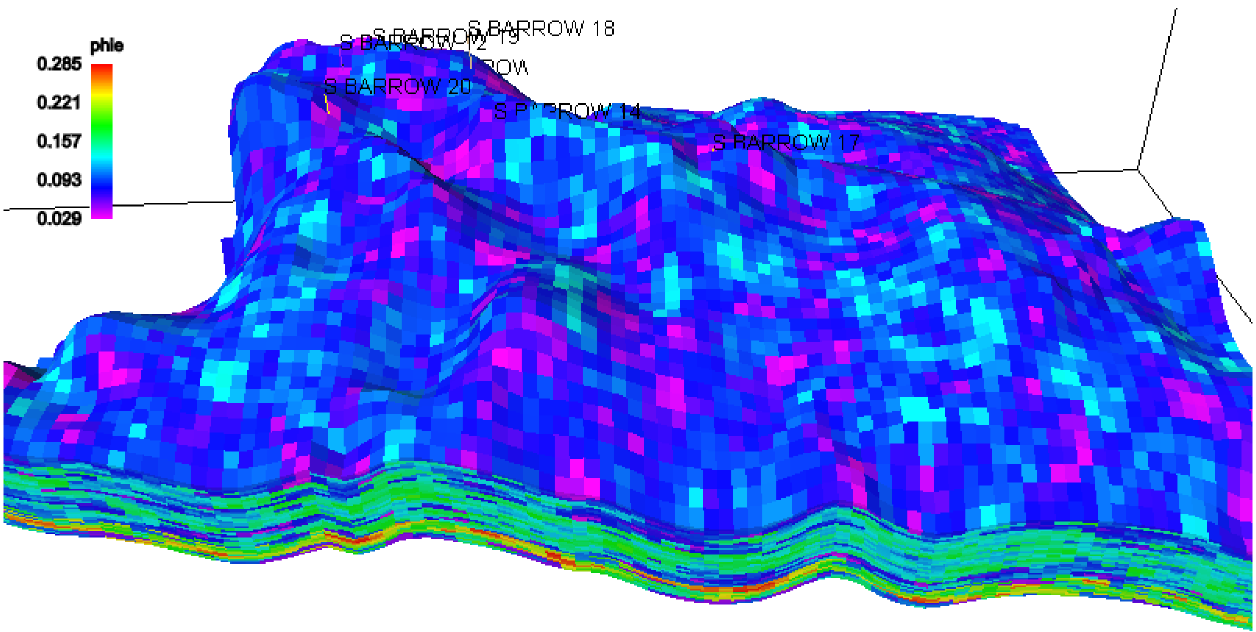

Figure 26: Porosity distribution in Barrow sands, RMS results.

The vertical porosity variation trend is clear in Figure 27 that shows an E-W cross section through the model.

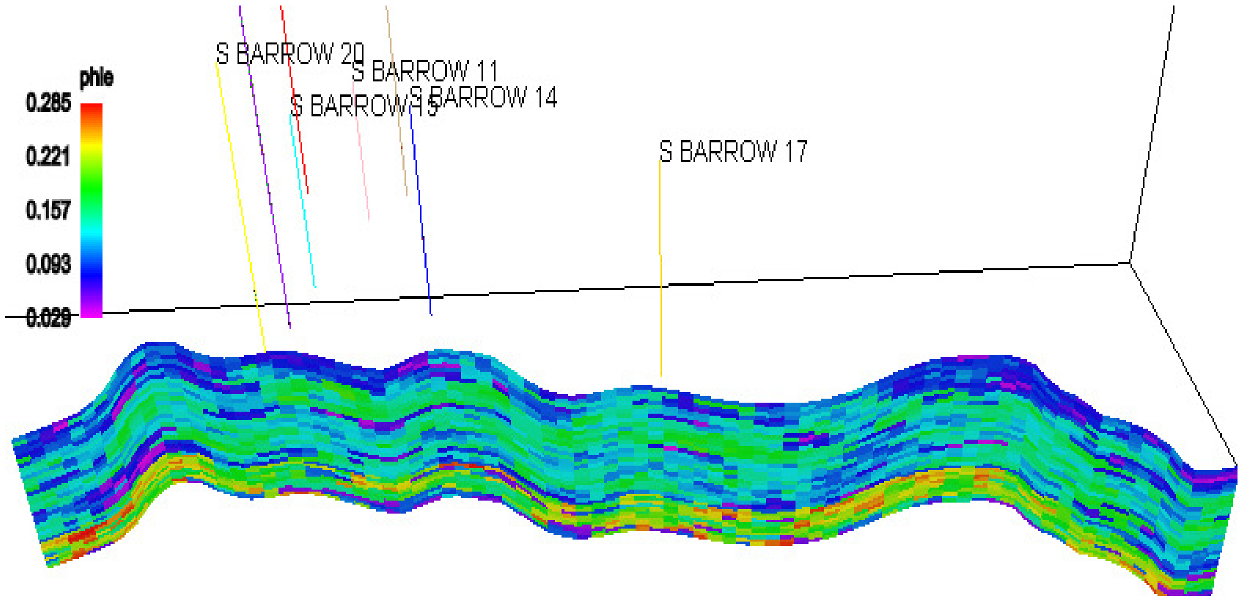

Figure 27: Porosity cross section through Barrow sands, RMS result.

Figure 28 shows permeability distribution. Figure 29 is an E-W cross section showing the vertical permeability distribution in the Barrow sands.

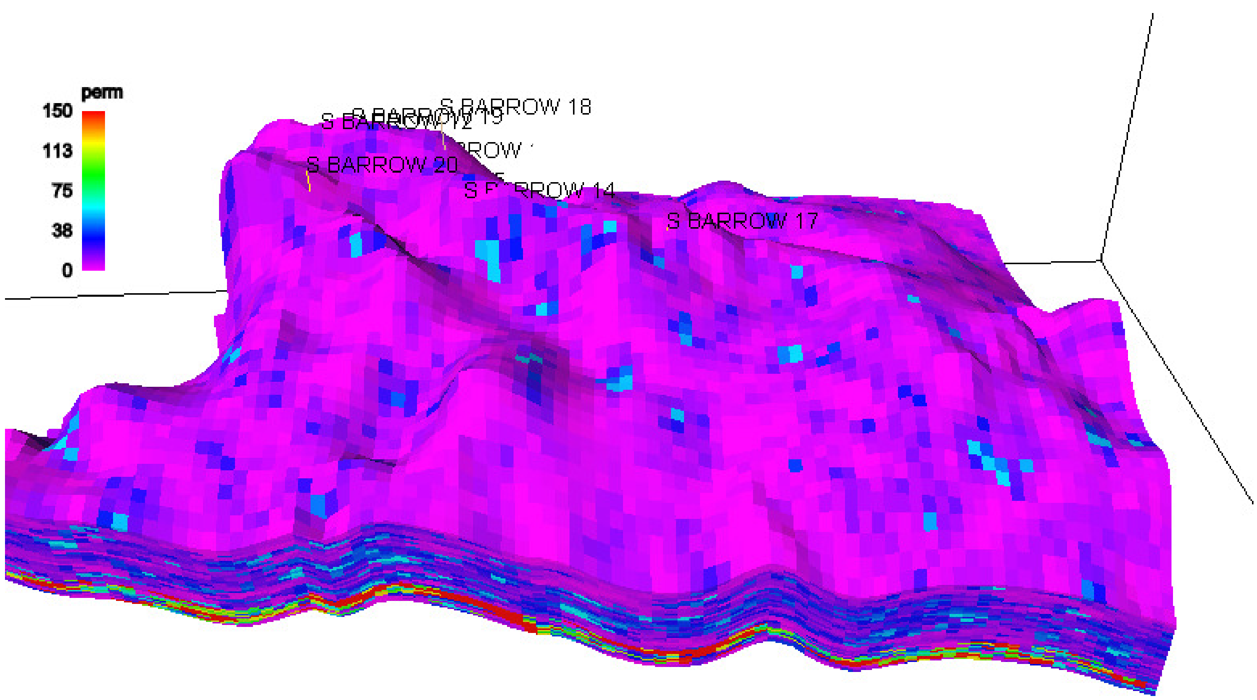

Figure 28: Permeability distribution in Barrow sands, RMS result.

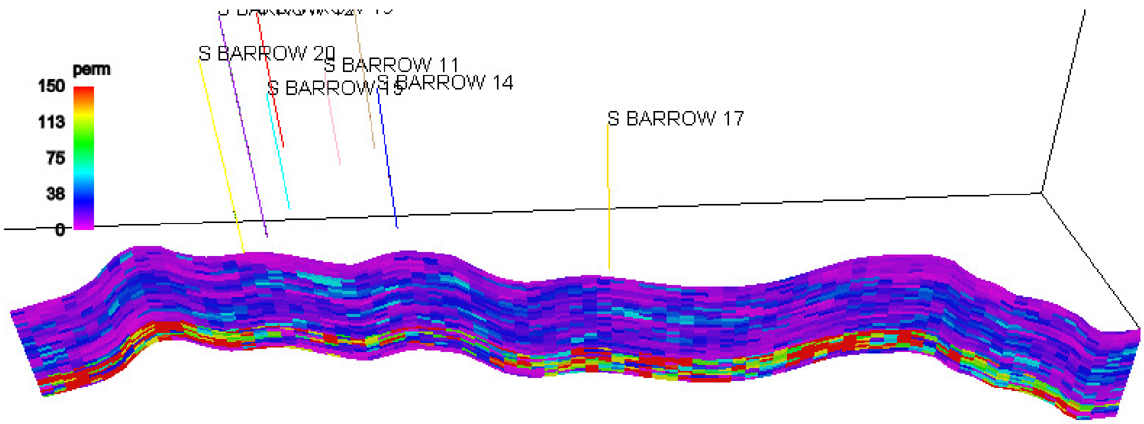

Figure 29: E-W cross section through the permeability model, Barrow sands.

<u>**Step 8**</u>. Creating CMG simulation model

Data scale up - The geological model that has been generated as described in the earlier section is comprised of small dimensioned grid cells (that match with the sampling frequency of the well logs). The geological model is typically not suitable for running flow simulations since it demands large run times for any practical application (in order of days to weeks of CPU time). To keep the run time in a manageable range the geological model is scaled up using a pressure solver. The concept of the scale up process is schematically shown in Fig. 30. Multiple grid cell of the geological model are thus represented by a single grid cell in the simulation grid. The pressure solver algorithm preserves the flow characteristics of the geological model (fine scale grid) in the simulation model.

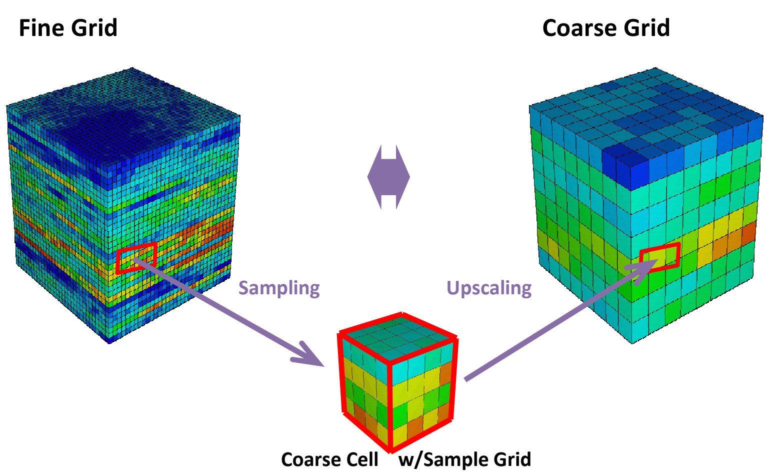

Figure 30: Schematic showing the scale up method.

Figure 31 is the RMS work flow used to upscale the geological model for the East Barrow field. The number of layers was reduced from 36 to 10. The X and Y direction dimensions of the grid cells were scaled up from 300 ft to 600 ft. The total number of grid cells was reduced from 287712 to 19980 for the East Barrow field.

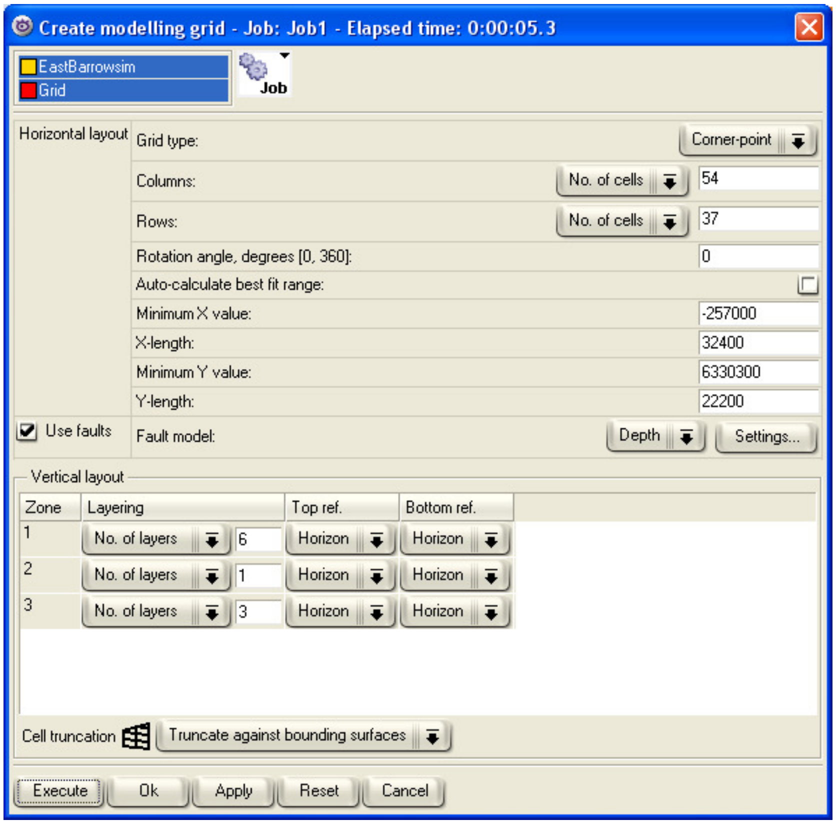

Figure 31: RMS work flow to scale up East Barrow fine scale model.

Figure 32 and Fig. 33 present the scaled up porosity and permeability data for East Barrow field respectively.

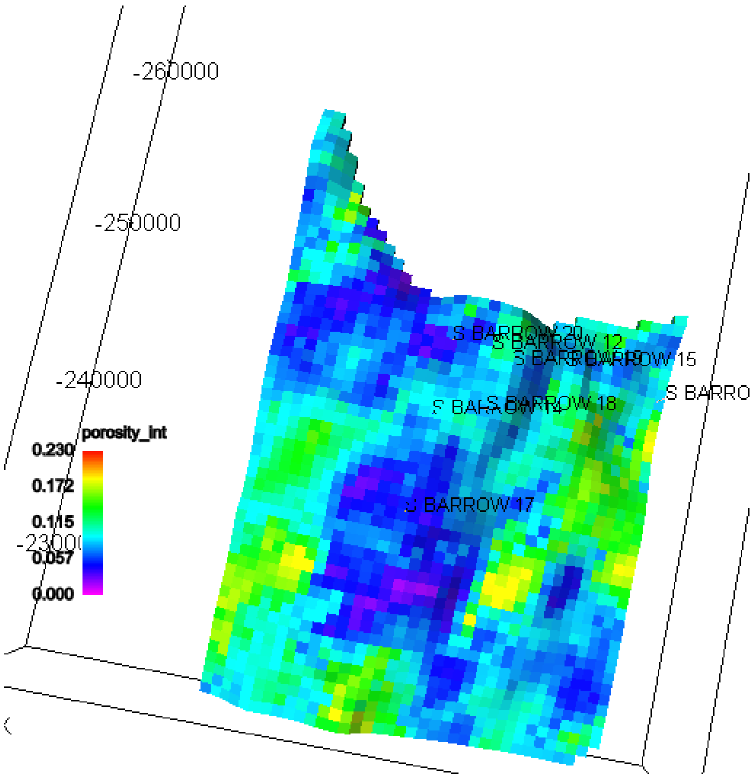

Figure 32: Scaled up porosity distribution for East Barrow.

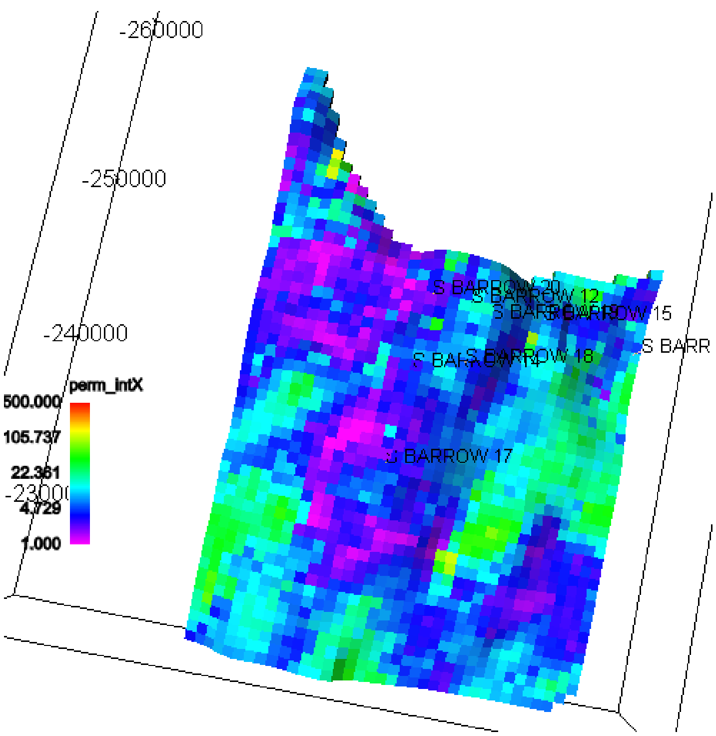

Figure 33: Scaled up permeability data for East Barrow field.

Temperature Distribution: A temperature parameter is generated for the East Barrow model based on the depth of the grid cell and the regional geothermal gradient. The temperature data is used to determine the hydrate stability interval in the East Barrow field. Figure 34 shows the grid cell depth of East Barrow model. Figure 35 shows the temperature distribution.

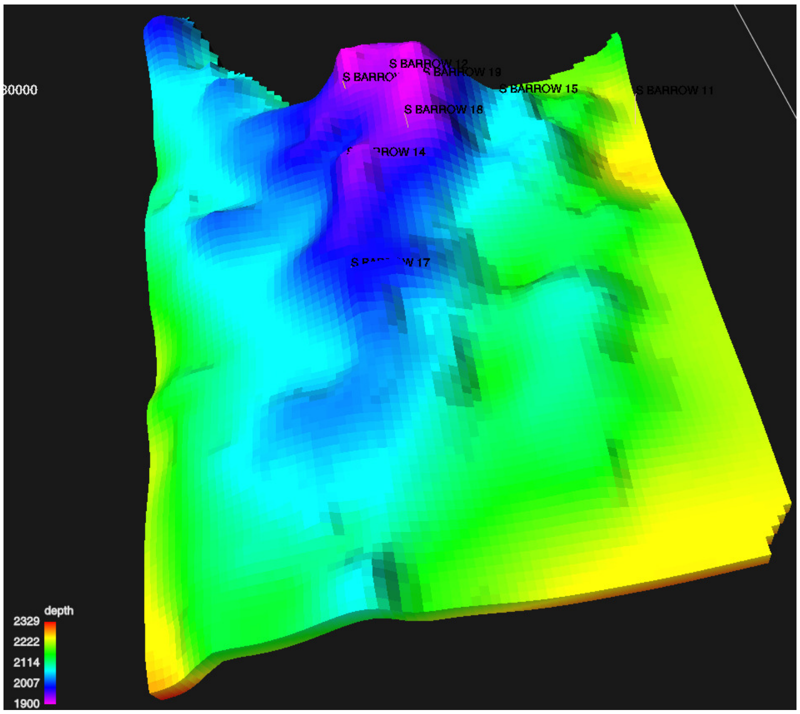

Figure 34: East Barrow model grid cell depth.

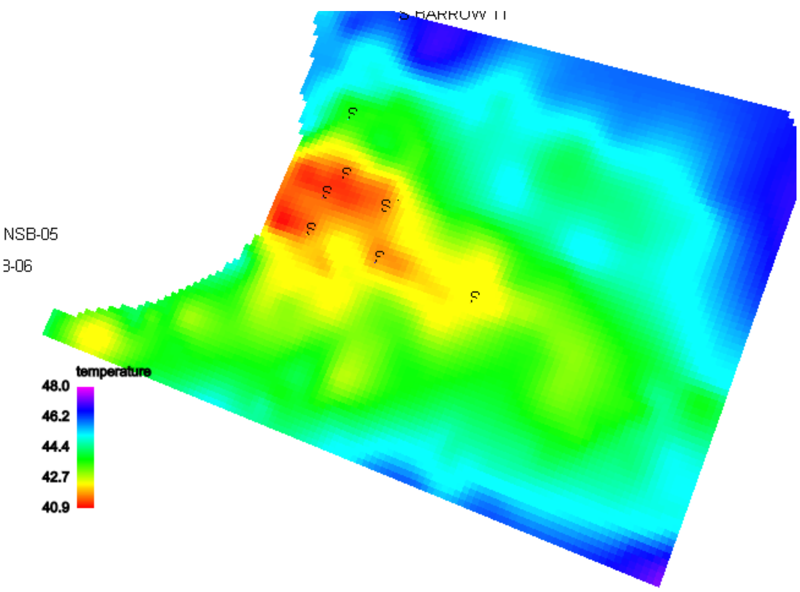

Figure 35: Temperature distribution in East Barrow, degree F.

Step 9: Water saturation distribution - Using the water saturation from core data and a water gas contact of 2081 ft sub-sea true vertical depth (sstvd) a water saturation parameter is generated in the East Barrow model. The depth of the grid cells presented in Fig. 35 is used as the reference depth. Figure 36 presents the water saturation distribution in the East Barrow field.

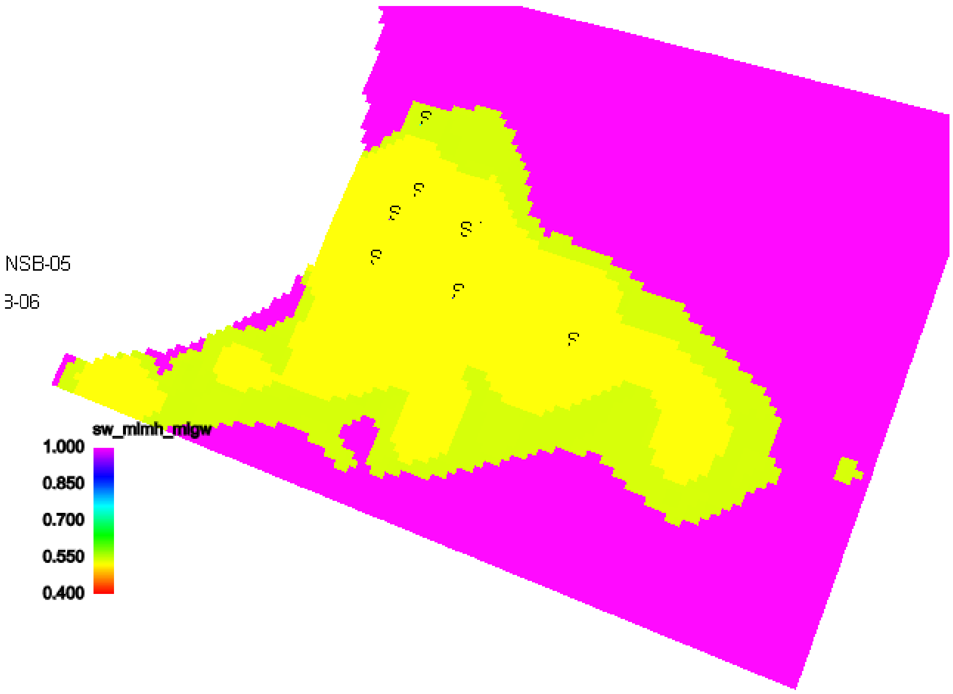

Figure 36: Water saturation distribution in the East Barrow field.

The reservoir parameters generated stochasticalled conditioned to the well log data (as described in the previous section) were exported into a CMG flow simulation model. Detailed history match and forecasting runs for the East Barrow field were performed. Several iterations were made to update the geostatistical model to achieve an accurate history match. A companion report presents the flow simulation work in details (Panda, Singh and Stokes, 2008).

RESERVOIR MODEL BUILD – Walakpa Gas reservoir

A flow simulation model (CMG) was constructed for studying the hydrate production characteristics in the Walakpa sands. First, a fine scale geological model was generated using RMS over the entire Walakpa sands. The petrophysical data was then scaled up to generate a simulation grid over the Walakpa gas field. The simulation data in CMG format was exported for flow simulation study.

Walakpa Geological Model:

We used the nine-step procedure described in the previous section to build the geostatistical model for the Walakpa field. The details of the model build process will be omitted (only the summary of the results are presented here).

Figure 37. presents the areal extent of the model. Well log data from nine wells, Walakpa 1, 2, 3, 4, 6, 7, 8, 9, and 10 was used to condition the geological model.

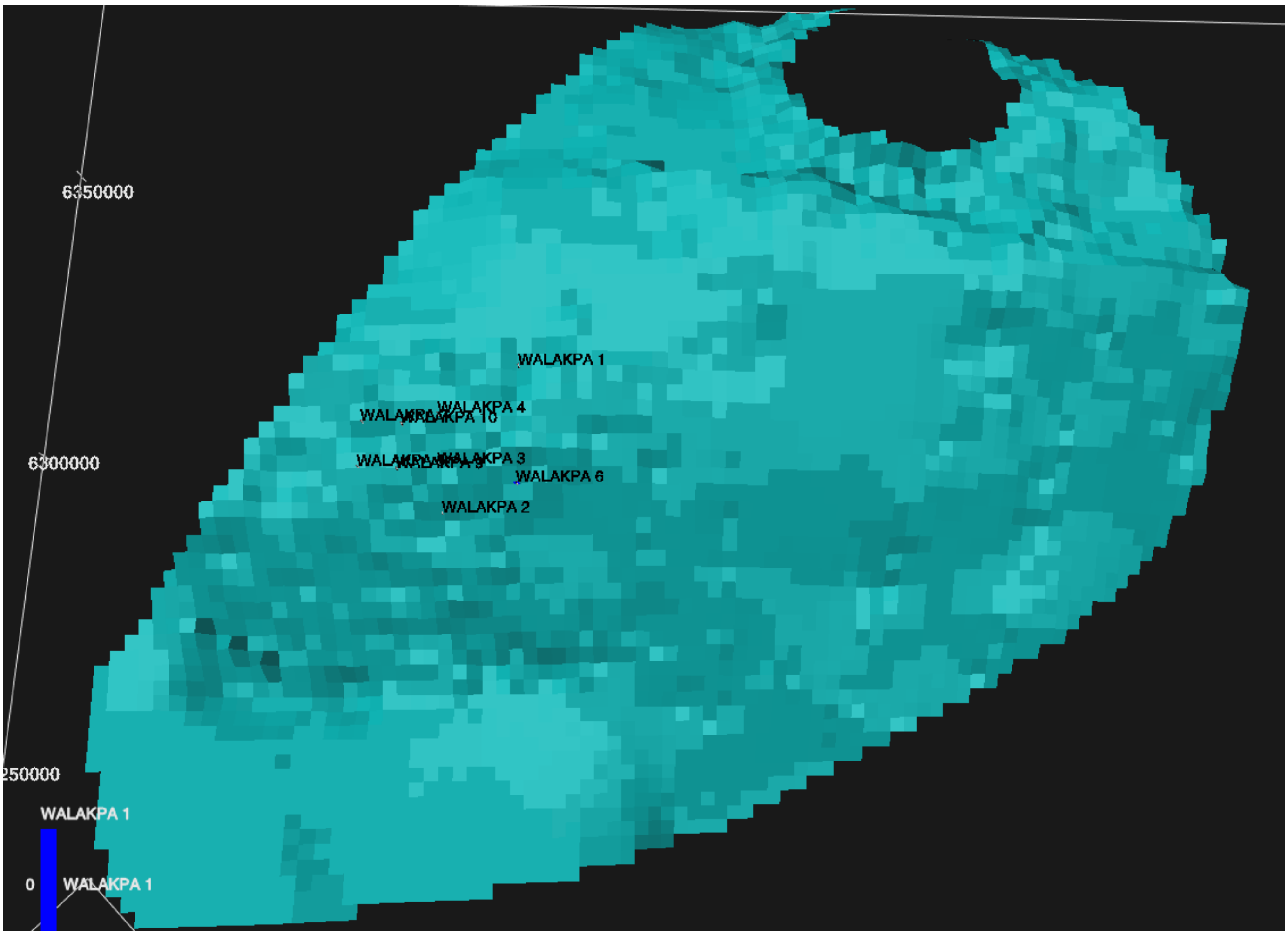

Figure 37: Areal extent of Walakpa geological model.

The geological model was constructed with cells of dimensions of 100 ft in X and Y directions and 2 ft in the vertical direction. Facies and petrophysical data were then generated. Figures 38, 39, and 40 present areal facies, porosity, and permeability distribution.

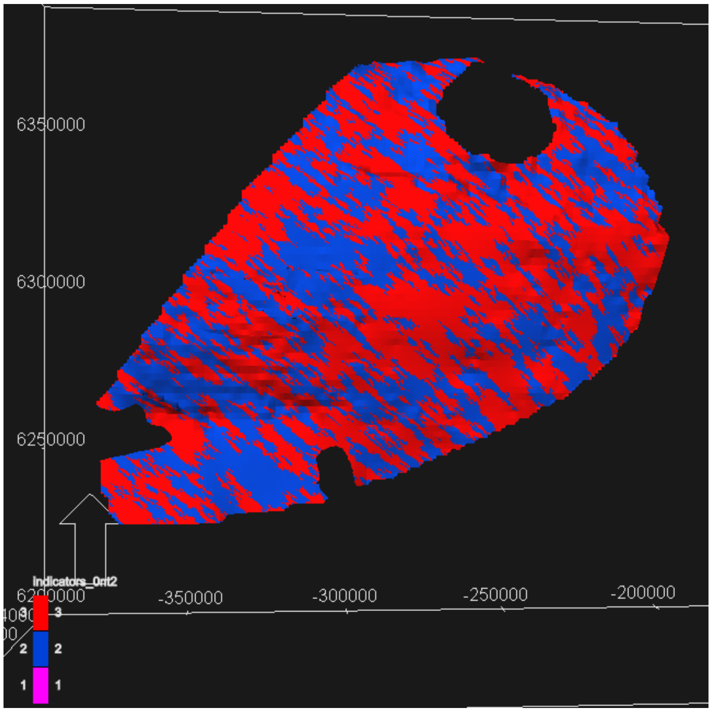

Figure 38: Facies distribution in Walakpa sands.

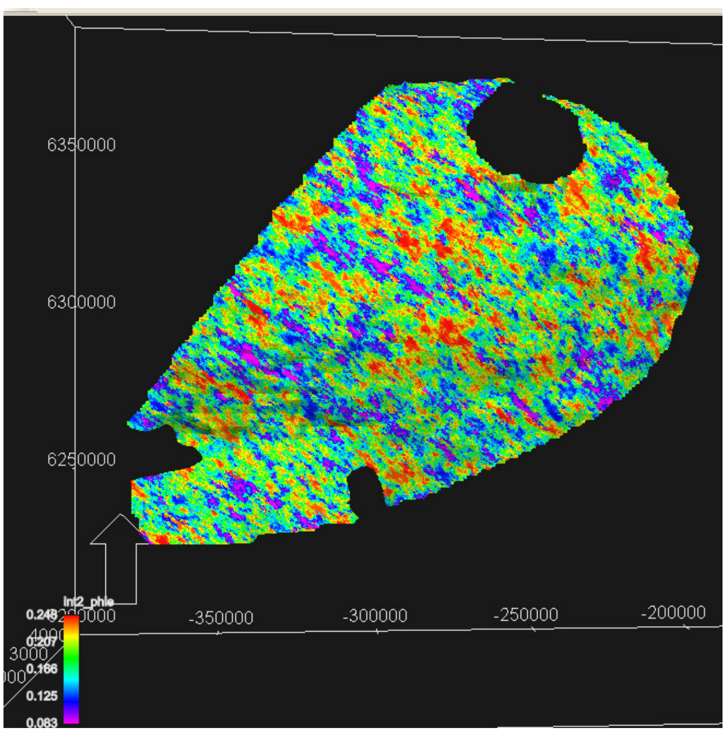

Figure 39: Porosity distribution in Walakpa sands.

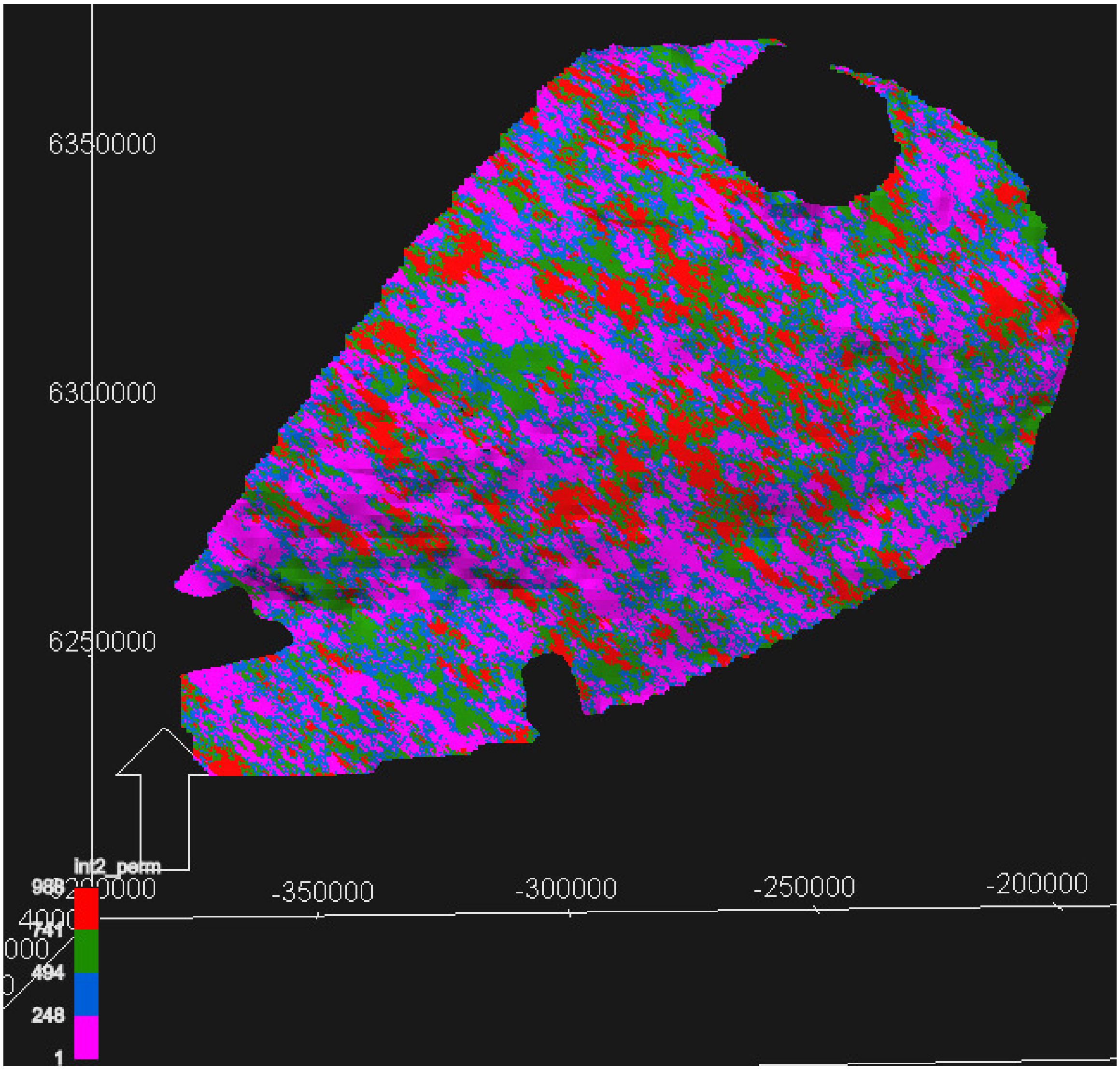

Figure 40: Permeability distribution in Walakpa sands.

A small subgrid over the Walakpa gas field was extracted for generating a simulation grid. Figure 41 presents the subgrid that covers the Walakpa gas field.

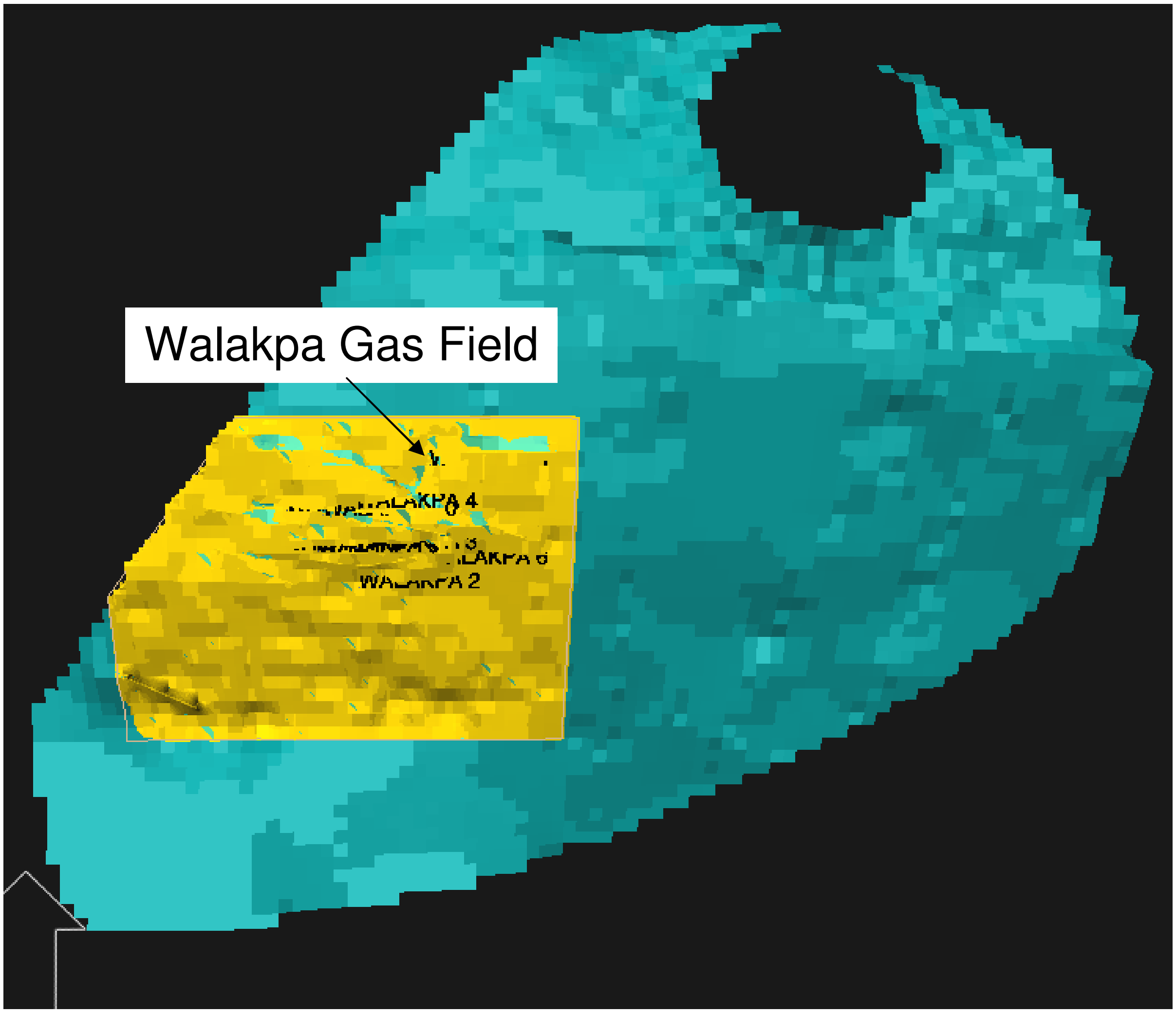

Figure 41: Sub-grid covering Walakpa gas field.

The fine scale petrophysical data was then scaled up to generate porosity, permeability, and water saturation data for the simulation model. Figure 42, 43, and 44 present the porosity, permeability, and water saturation data for the Walakpa gas reservoir. The simulation data was exported in CMG format for flow simulation study.

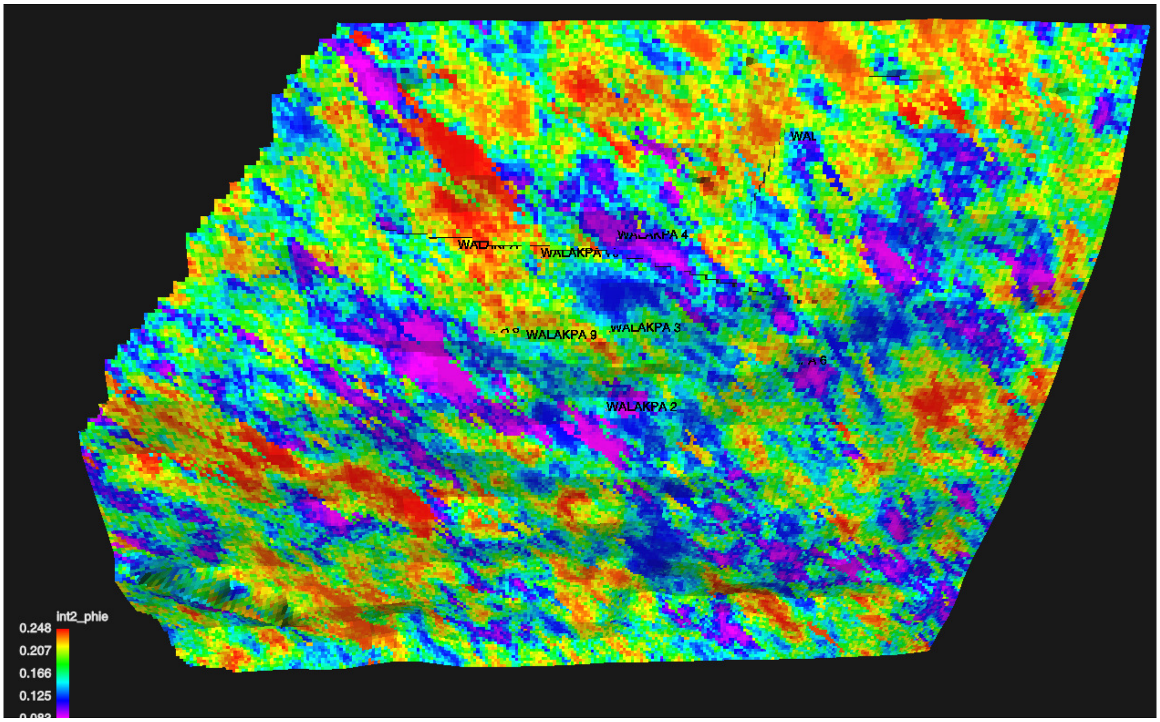

Figure 42: Porosity distribution in Walakpa reservoir.

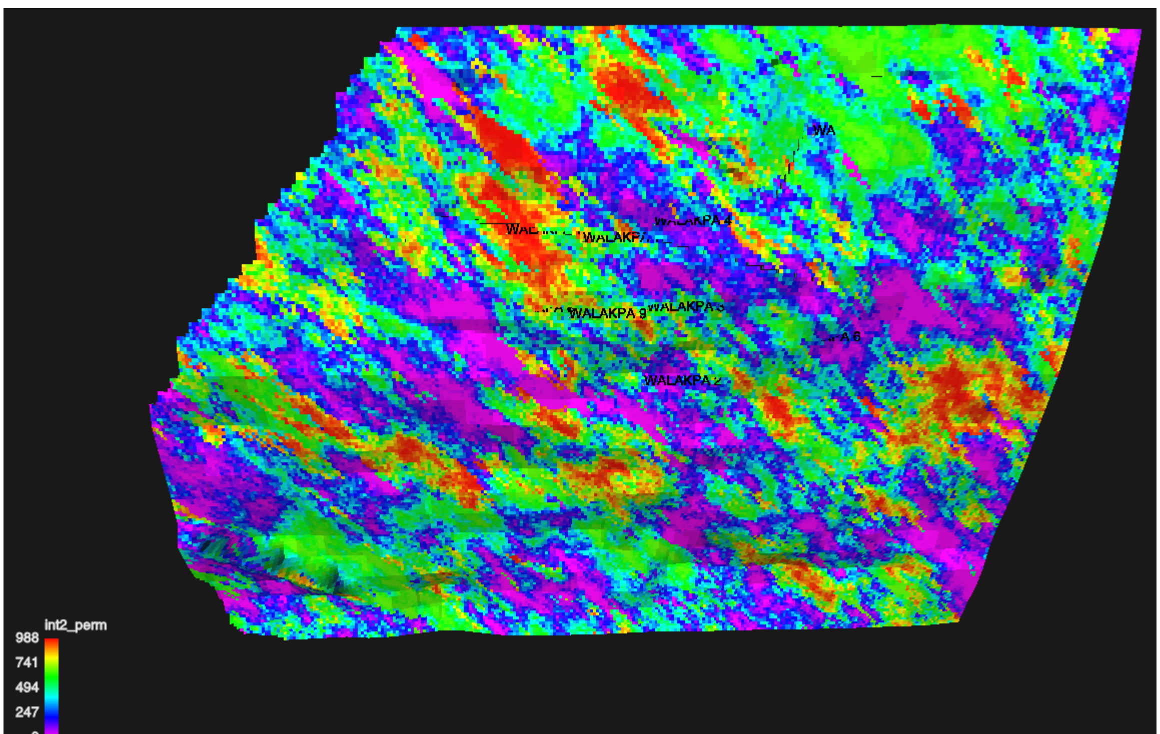

Figure 43: Permeability distribution in Walakpa reservoir.

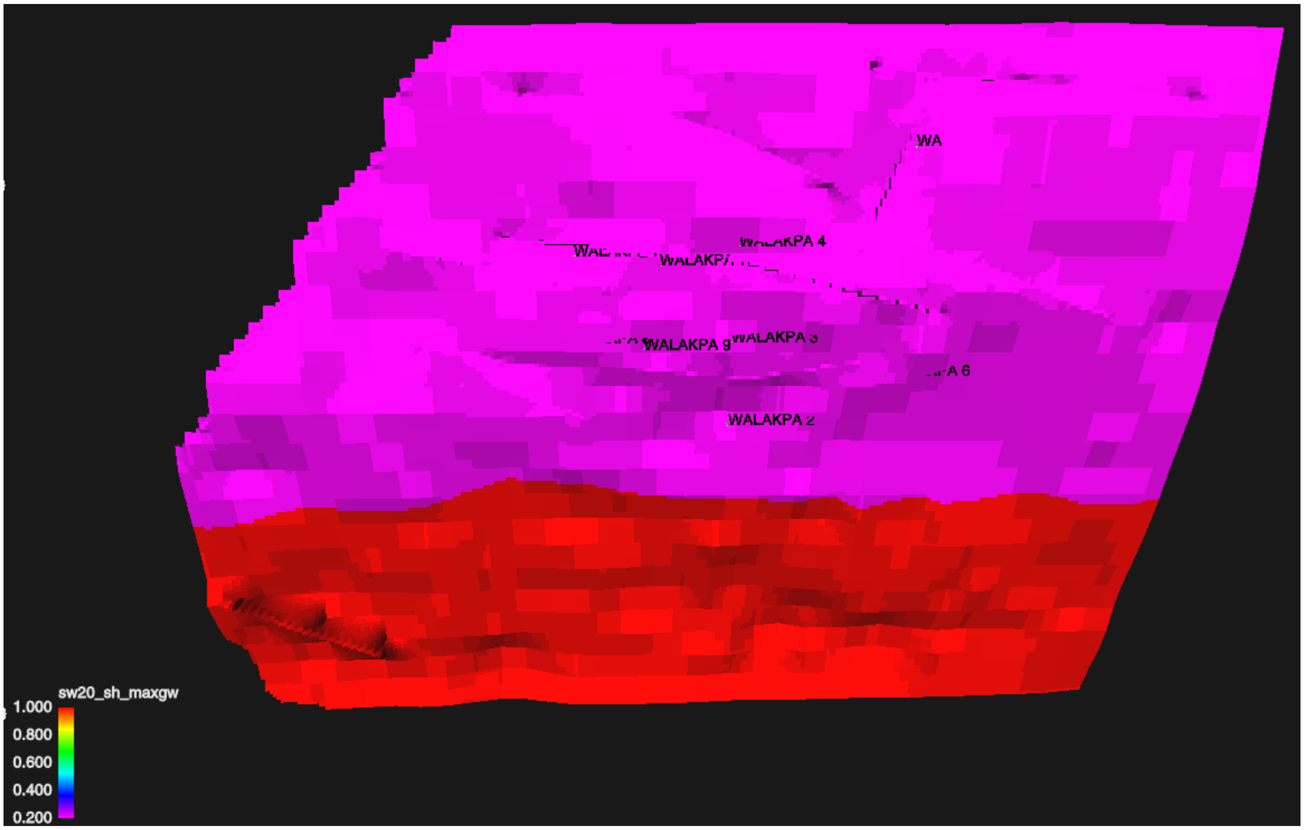

Figure 44: Water saturation distribution in Walakpa reservoir.

CONCLUSIONS

An integrated fine scale 3D geological model has been constructed for the Barrow and Walakpa gas reservoirs. Data from multiple sources, such as seismic data, geological information, well log data, core data, and pressure build up analysis are integrated using a geostatistical technique to build the models. The fine scale models are consistent with the well log data and the geological information. The geological models are upscaled to build flow simulation models to study the hydrate dissociation mechanism in the East Barrow and Walakpa field.

REFERENCES

1. Bird, Kenneth J.: *"Alaska: A Twenty-First-Century Petroleum Province"*, 2001, AAPG Memoir 74, P. 137-165.

2. Grantz, Arthur; Clark, D.L.; Phillips, R.L.; and Sirvastava, S.P.: *"Phanerozoic stratigraphy of Northwind Ridge, magnetic anomalies in the Canada basin, and the geometry and timing of rifting in the Amerasia basin, Arctic Ocean"*, 1998, GSA Bulletin, V. 110, No. 6, P. 801-820.

3. Houseknecht, David W. and Bird, Kenneth J.: *"Sequence stratigraphy of the Kingak Shale (Jurassic-Lower Cretaceous), National Petroleum Reserve in Alaska"*, 2004, AAPG Bulletin, V. 88, No. 3, P. 279-302.

4. Houseknecht, David W. and Bird, Kenneth J.: *"Oil and Gas Resources of the Arctic Alaska Petroleum Province"*, 2005, USGS Professional Paper 1732-A.

5. Kimyai, Abbas: *"Palynology and Biostratigraphy of the Lower Cretaceous Sediments in the South Barrow Test Well No. 1, Point Barrow, Alaska"*, 2000, Palynology, V. 24, P. 201-215.

6. Kirschner, C.E.; Grantz, Arthur; & Mullen, M.W.: *"Impact Origin of the Avak Structure, Arctic Alaska, and Genesis of the Barrow Gas Fields"*, 1992, AAPG Bulletin, V. 76, No. 5, P. 651-679.

7. Morahan, G.T.; Greet, D.N.; & Walsh, T.P.: "*Seismic and Well Log Evaluation of the Barrow High Area, Including the Walakpa and Barrow Gas Field",* 2008, under DOE Project Number DE-FC26-06NT42962

7. Nelson, Philip H. and Bird, Kenneth J.: *"Porosity-Depth Trends and Regional Uplift Calculated from Sonic Logs, National Petroleum Reserve in Alaska"*, 2005, USGS Scientific Investigations Report 2005-5051.

8. Opstad & Associates, 1989,: "*Thin Section and Special Core Analysis of the Barrow Sandstone in NSB Well #6",* technical report prepared for North Slope Borough Gas Development Project, Alaska.

9. Peters, K.E., Bird, K.J., Keller, M.A., Lillis, P.G., and Magoon, L.B.: *"Distribution, Richness, Quality, and Thermal Maturity of Source Rock Units on the North Slope of Alaska"*, 2003, USGS Open-File Report 03-328.

National Energy Technology Laboratory

626 Cochrans Mill Road
P.O. Box 10940
Pittsburgh, PA 15236-0940

3610 Collins Ferry Road
P.O. Box 880
Morgantown, WV 26507-0880

One West Third Street, Suite 1400
Tulsa, OK 74103-3519

1450 Queen Avenue SW
Albany, OR 97321-2198

2175 University Ave. South
Suite 201
Fairbanks, AK 99709

Visit the NETL website at:
www.netl.doe.gov

Customer Service:
1-800-553-7681